LUÍS DIAS[1] FRANK BRAUNSCHWEIG[2]
NUNO GROSSO[3] HUGO COSTA[3] PEDRO GARRETT[3]

FLOOD RISK MAPPING

METHODOLOGICAL GUIDE

1. Climate Change Impacts Adaptation and Modeling research group – FC-UL. Bolseiro de Doutoramento da Fundação para a Ciência e Tecnologia com a referência SFRH/BD/70435/2010.
2. Action Modulers, Consultores de Segurança S.A. Marine Environment and Technology Center (Maretec) – IST-UL.
3. Climate Change Impacts Adaptation and Modeling research group.

TABLE OF CONTENTS

FIGURES INDEX

TABLES INDEX

INTRODUCTION

"Water, taken in moderation, cannot hurt anybody."

Mark Twain

Floods are part of one of several natural hazards to which contemporary society is exposed to, being one of the main phenomena responsible for human, economic and environmental loss in the global context (Schmidt-Thomé et al., 2006, EEA et al., 2008). These are responsible for a third of the economic losses as a result for natural disasters in Europe, the most frequent type of events, along with windstorms (EEA et al., 2008). With the growing awareness of the dangers and damages associated in line with the increase in the number and magnitude of extreme precipitation events (Bladé et al., 2010, Kharin et al., 2007, Santos and Miranda, 2006, Dias, 2013, Vicente-Serrano et al., 2011), it is necessary to deepen scientific knowledge in this interdisciplinary context where climate change (Pall et al., 2011, Min et al., 2011, IPCC, 2013, IPCC, 2012), risk assessment and the creation adaptation strategies contribute to increase resilience to these type of phenomena.

These concerns have been increasingly being taken into consideration by the insurance sector, which has been making more and more significant investments in assessing and controlling the risk of flooding (e.g. Leurig and Dlugolecki, 2013, Kron, 2005, Thieken et al., 2006).

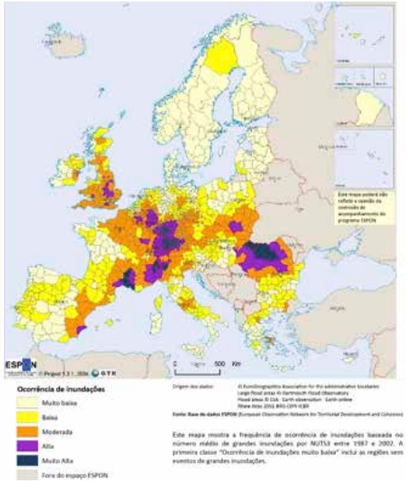

Figure 1. *Frequency of occurrence of floods in the European Union. Source: adapted from Schmidt-Thomé et al. (2006)*

It is in this context that the research project "Flood Risk and Vulnerability Mapping in Climate Change Scenarios" (CIRAC) in partnership with the Portuguese Association of Insurers and the research group *Climate Change Impacts Adaptation and Modelling* (CCIAM), Faculty of Sciences University of Lisbon.

This paper has been developed within this project and is part of a PhD thesis in progress with the interim title "Climate change, flooding and the city. Contributions to the study of urban resilience in situations of torrential rain."

The results of the hydrological modeling presented in this paper were also obtained under CIRAC project, a partnership between the company Action Modulers S.A and CCIAM using an integrated version of MOHID Land and *Storm Water Management Model* programs.

The purpose of this paper consists of presenting a methodology that allows quantifying the risk of flooding associated with the built environment embodied in buildings. There are, however, specificities that will determine the methods of analysis, namely the size of the basin and the type of flooding that occurs there. Not being able to treat all cases, the approach presented here focuses on flash floods in small basins. The proposed method can be used to assess the risk of flood in climate change scenarios. However and due to the complexity of the necessary procedures to obtain data from extreme rainfall resulting from models that perform these scenarios, it was decided not to include this process in this guide.

The first part of this paper is dedicated to the main concepts related to the evaluation of flood risk, whose domain is critical for understanding the remaining content of the paper.

The second part presents the methodological procedures for the assessment of flood risk. This assessment starts with the necessary processes for defining probabilities of occurrence associated with the phenomena of flooding and then addressing strategies aimed at optimizing the hydrodynamic modeling to obtain flooded areas and other characteristics of the flood.

Finally we propose a method to quantify flood risk based on the annual average damage for different damage categories. In this last part it is also proposed to integrate the different damage categories in a single indicator with the purpose to conduct a comprehensive reading of the risk that a particular area is exposed to.

CONCEPTS

"We forget that the water cycle and the life cycle are one."

Jacques Yves Cousteau

floods

Flood consists of the overflow of a watercourse from its natural bed, and it can be slow or fast. The flow resulting from a considerable precipitation with a duration of several days or weeks is considered progressive while the fast flooding occur as a result of extreme rainfall and usually of short duration. Floods also include the sinking of land as a result of rising groundwater or overloaded drainage systems (Julian et al., 2009).

According to Community Directive 2007/60/EC on the assessment and management of flood risks and in the meantime transposed into national legal system, the flood is defined as a "temporary covering by water of land not normally covered by water", where "is included floods from rivers, mountain torrents and the Mediterranean ephemeral water courses, and floods from the sea in coastal areas" and it may be "excluded floods from sewerage systems origin".

This definition is implemented into national reality by Decree-Law No. 115/2010, where the flooding comprises "temporary covering by water of a parcel of land outside the normal bed, resulting from floods caused by natural phenomena such as rainfall, increasing of the flow of rivers, mountain streams and ephemeral water courses corresponding to these river floods, or super elevation of the water level of the sea in coastal areas."

exposure

The exposure is the presence of people, goods or other items potentially subject to damage in areas where flooding occurs (see e.g. UNISDR, 2004 UNISDR, 2009 SEC, 2010) and can be quantified by the number or value of the elements found within this area (Merz et al., 2007). Thus, a certain very fragile element to flooding but that is not exposed to this phenomenon, will always have a zero risk (Bruijn et al., 2009).

susceptibility

In the context of a related flood study, the concept of susceptibility has several interpretations. For some authors susceptibility comes down to the predisposition of a given area to be affected by these phenomena. This assessment takes into account physical factors of the land, and does not include the probability of occurrence of floods (Julian et al., 2009).

With greater relevance to the assessment of flood risk, the concept of susceptibility is also applicable to the elements affected by a flood. In this case, the concept refers to the process of generation of damage, being dependent on one or more characteristics of the flood and the constitution of the affected elements (Schanze, 2006).

vulnerability

The word vulnerability refers to the characteristics that define the greater or lesser capacity of an element (population or active) to resist when exposed to a flood event (Schanze, 2006). The vulnerability comprises susceptibility, exposure and value of elements (EXCIMAP, 2007), which may be expressed in tangible, intangible, direct and indirect effects caused over the element or set of elements under analysis (Dutta et al., 2003).

risk

Risk is defined generically as the probability of damaging consequences or losses (death, injuries, property, means of production, disruptions in economic activities or environmental impacts) that result from the interaction between the natural environment or human induced hazards and the conditions of vulnerability of elements (UNISDR, 2004, ISO 31010, 2009).

flood risk

The concept of flood risk is formally defined in both the European and national standards consisting, according to Decree-Law No 115/2010 establishing a framework for the assessment and management of flood risks, of the "combination of the probability of flooding taking in account its magnitude, and the potential adverse consequences to human health, the environment, cultural heritage, infrastructure and economic activities, and their damaging consequences accessed by identifying the number and type of affected activity, may sometimes be supported by a quantitative analysis." That is, it is necessary to examine the floods using different probabilities of occurrence, establishing the characterization of the elements exposed and, whenever relevant, proceed to the actual quantification of the risk of flooding.

The calculation of the flood risk is quite stabilized in literature, consisting of the product of the consequence of flooding and its probability of occurrence (UNISDR, 2004, Meyer et al., 2009c, Gouldby and Samuels, 2005).

$$\text{Risk} = \text{Consequence} \times \text{Probability} \quad (1)$$

The Probability reflects the frequency that an event with a certain magnitude occurs. When assessing the flood risk this concept is usually translated by the return period, which corresponds to the inverse value of the occurrence and it is equal to the average number of years between two events of equal magnitude.

The consequence is defined in different ways by different authors, consisting of the potential hardship caused by the flood and taking into account the factors of vulnerability of the elements and magnitude of events (Kron, 2005 UNISDR, 2004 EXCIMAP, 2007).

Based on the approach of the *International Strategy for Disaster Reduction* that the United Nations uses to evaluate the Risk, consequences are assessed through the equation (2).

$$\text{Consequence} = \text{Value} \times \text{Susceptibility (magnitude)} \times \text{Exposure} \quad (2)$$

Where the value of the elements is usually expressed in monetary units or the number of human lives;

The susceptibility, as previously mentioned, expresses the creation of damage, which depends on the characteristics of the flood (magnitude of the event) and may

lie in the range between 0% (not susceptible) and 100% (maximum susceptibility);

And the Exposure corresponds to the presence or absence of the element at the time of the event, being a binary parameter which can assume the value of 0 (not exposed) or 1 (exposed).

The criteria of Value, Susceptibility and Exposure are vulnerability parameters of the elements and the magnitude of flooding is a feature that is leading to potential damage that can be caused by a particular event. The relation between the susceptibility and the magnitude of the event is usually expressed through damage curves for the calculation of the risk. These relations are critical in quantifying the risk of flooding, being this a theme developed throughout this work[i].

As mentioned, the theorization of the risk can be presented in several ways, such as the example formulation presented by the European Commission in its guidelines for the assessment and mapping of risk (see SEC, 2010). In this paper risk is defined as the function of the product among the probability, exposure and vulnerability.

$$\text{Risk} = \text{Probability} \times \text{Exposure} \times \text{Vulnerability} \quad (3)$$

In this case, Exposure and Vulnerability are parameters that define Consequence according to what is illustrated in function (1), varying the concept of vulnerability previously presented, since it excludes the exposure of its formulation, containing however both value and susceptibility.

i *see for example the section Damage Curves.*

Both ways of accounting the presented risk allow obtaining the same results, in spite of differences in the steps of the calculations. In this guide it was adopted the approach of the United Nations with minor modifications discussed further on.

return period

The return period consists of the probability of repetition of a flood with a determined magnitude, and is generally defined as the average number of years between the occurrences of two successive events with an identic magnitude (Andrade et al., 2006). Return periods, which reflect a probability of occurrence, are related to the probability of exceedance obtained from equation (4), where p is the probability of exceedance and T the time, which is usually set in years.

$$p = \frac{1}{T} \quad (4)$$

In this context the probability of exceedance is directly related with the probability that an event of a certain magnitude has to be exceeded. With inverse meaning the probability of non exceedance can also be obtained, by using the equation (5) where p and T correspond respectively to the probability and time.

$$p = 1 - \frac{1}{T} \quad (5)$$

Table 1 presents the most common return periods in hydrologic studies and correspondent probabilities.

Table 1. Return periods and probabilities.

Return period in years	2	5	10	20	50	100	500
Probability of exceedance	0.5	0.2	0.1	0.05	0.02	0.01	0.002
Probability of non exceedance	0.5	0.8	0.9	0.95	0.98	0.99	0.998

hyetographs

The Hyetographs describe how the precipitation of a given event can be distributed over time. It is used for its composition intensity curves-duration-frequency (IDF) which characterizes the relation between the intensity and duration of precipitation for a given frequency which is defined by the return period. This characterization is published by Brandao et al. (2001) in regards to 27 udometric meteorological stations in mainland Portugal where necessary parameters are defined for the definition of these hyetographs for precipitation with different durations and return periods. Brandão et al. (2001) found that the potential curves are the type that best fit the relation between the intensity and duration for a given return period in mainland Portugal.

Equation (6) presents the theoretic formulation of the equation of this curve, where I describes the intensity defined in mm/hour, D a duration in minutes, a and b are parameters of the IDF curve.

$$I = aD^b \quad (6)$$

These authors also reported breaks in the rainfall intensities for different durations resulted from different meteorological processes that are at their origin. In this manner three stretches are defined (lasting 5 to 30 minutes, from 30 minutes to 6 hours, 6 to 48 hours) in the IDF curves for a given return period for a determined weather station.

Table 2 presents the parameters of the IDF curves for the station of the Geophysical Institute of the Infante D. Luis (IGIDL), located in the botanical garden of the Faculty of Sciences in Lisbon.

Table 2. Parameters a and b of IDF curves for different return periods and duration for Lisbon (IGIDL). Source: Brandão et al. (2001).

Return period (years)	2		5		10		20		50		100		500	
Parameters	a	b	a	b	a	b	a	b	a	b	a	b	a	b
From 5 to 30 minutes	176.46	-0.529	214.32	-0.499	239.69	-0.486	264.16	-0.477	295.96	-0.467	319.86	-0.461	375.21	-0.451
From 30 min. to 6 hours	251.82	-0.628	345.32	-0.634	407.36	-0.637	466.92	-0.639	544.07	-0.641	601.92	-0.642	735.65	-0.644
From 6 to 48 hours	362.78	-0.698	545.58	-0.721	670.81	-0.732	792.97	-0.739	953.23	-0.747	1074.5	-0.752	1357.3	-0.76

hydrologic modeling

Hydrological models consist of the simplified representation of part of the hydrological cycle. Its goal is to simulate a certain reality for purposes of prediction or understanding its behaviour. These models require information on rainfall and runoff[ii] for the study area which is typically a basin or sub-basin area. The hydrological models present the water balance for each cell in a given grid for each time period and for each section of the waterline.

Using these methods and to run flood risk maps, it is necessary to transform the values of discharge in flood levels. There are some solutions for this purpose, with hydrodynamic models such as 1D, 2D and 3D (EXCIMAP, 2007).

The 1D model is typically used to model the rivers channels and urban drainage networks. Such models describe the change of a certain variable (e.g. water flow or sediment concentration) in a unique horizontal direction (*x* or *y*). 2D models shape variables in two horizontal dimensions (*x*, *y*). These models calculate the speed of flows, propagation, duration and rise in the water level. Lastly, 3D models calculate variables in analysis both in horizontal and vertical dimensions (*x*, *y*, *z*) - Figure 2. These models are useful for modeling floods in basins where soil has different characteristics upright and that may influence the phenomenon of flooding under study (MRC / WUP-FIN, 2008 Trancoso et al., 2009).

ii *If these values do not exist, it may be extrapolated through techniques of regionalization.*

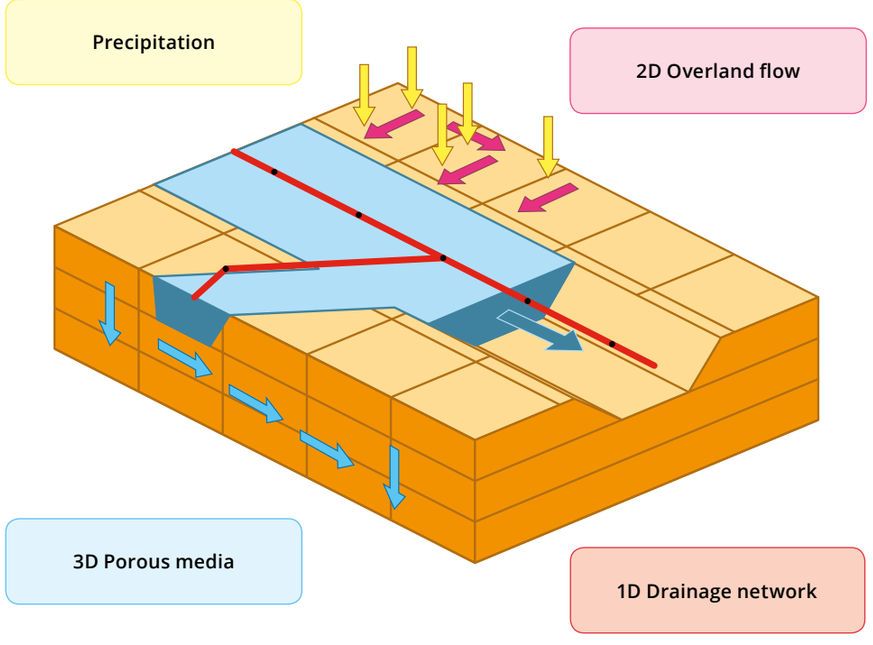

Figure 2. *Schematic representation of 2D and 3D models. Source: Trancoso et al. (2009).*

damage curves

The damage curves consist of mathematical expressions relating a flood characteristic (eg, depth, speed, duration, etc) with the damage potentially caused by this same feature in the elements. That is, these curves represent the susceptibility of the exposed elements as a result of the magnitude of the flood event.

The damage curves are usually obtained using the information loss caused by floods with certain characteristics observed in the past. There are, however, other ways to obtain it, such as resistance tests of materials in laboratory, or by resorting to experts for their empirical formulation (Dutta et al. 2003 EXCIMAP, 2007 Schanze et al. 2006).

The relation between magnitude of the event and susceptibility of the exposed elements is present in the different categories of damage resulting from a flood event.

Table 3. *Damage categories and examples (damage category studied is highlighted in blue). Source: Dutta et. al. (adapted), 2003.*

CLASSIFICATION			EXAMPLES
Tangibles	Direct	Primary	Structures, assets and stocks
		Secondary	Environment recovery
	Indirect	Primary	Interruption of production
		Secondary	Regional and national economic impact
Intangibles			Population - Health and psychologic damages

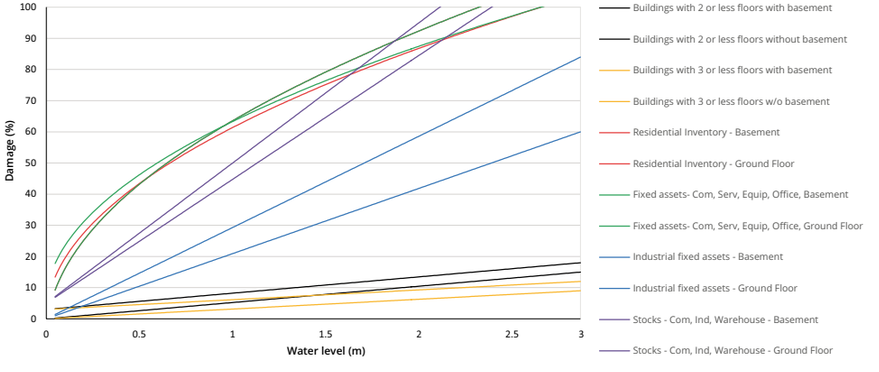

Figure 3. *Damage curves -depth for tangible damages, direct, primary. Sourcee: adapted from Markau (2003), Reese et al. (2003), Meyer and Messner (2005) e Sterr et al. (2005).*

The main damage categories are divided into tangible and intangible losses. Tangible damages can be expressed in monetary values or percentage of damage and are subdivided into two subcategories: direct and indirect damages (Table 3). Of these, the primary direct tangible damages will be those whose approach will be further detailed in this guide.

Figure 3 presents the damage curves adopted in this work for the risk assessment. These curves relate the depth of the flooding with primary direct tangible damage, being divided into the building structure, residential inventory, fixed assets and stocks.

probability-damage curves

Risk assessments using the curves that relate the probability of exceedance of the losses, or the return period with the correspondent damage are particularly important because they allow risk stratification and developing strategies for their reduction (IPCC, 2012). The use of these curves provides the average annual damage from a certain area or exposed element (Meyer et al., 2009b).

When calculating damage for a probability of exceedance (P_i), we only obtain the values of the damage (D) for an episode of flooding with a particular characteristic. This calculation represents a point on the probability-damage curve corresponding to the risk for this return period after applying the formula given in equation (1).

By performing this calculation for different return periods we obtain different points of the curve that by adjusting a function (for example polynomial, exponential, etc.) to these points and their linear interpolation, result in the damage-probability curve.

The area under this curve provides the average annual damage from the elements exposed under study. The calculation of this area can be achieved in different ways such as by calculating the integral of the function describing the curve[iii], although it is more usual to use the formulas (7) and (8) to obtain a closer figure for that area, where $\bar{D}$ corresponds to the average annual damage or risk, (D_i) to the average damage from two known points on the curve and to the probability of the interval between these two points (Meyer et al., 2009a)

$$\bar{D} = \sum_{i=1}^{K} D[i] \times \Delta P_i \qquad (7)$$

$$D[i] = \frac{D(P_{i-1}) + D(P_i)}{2} \qquad (8)$$

The probability damage curve will be as less uncertain as higher the number of return periods analyzed will be, since it is assumed that the damages present a linear behaviour between two known points on the curve. Usually there is an overestimation of the damage when comparing a curve obtained by analyzing six return periods (eg 2, 5, 10, 20, 50, 100 years) with another which damages are accounted for all return period between year 1 and 100 (eg 1, 2, 3, ..., 98, 99, 100 years).

However, decreasing the uncertainty of these curves is limited by the time required to obtain the information of damage of the amount of return periods analyzed, and the ability of hydrological models to produce the necessary detail to show such minor differences in rainfall associated with these return periods (Ward et al., 2011).

iii *In order to calculate the integral of the curve represented in Figure 4 it is necessary to transform the coordinate axis in a linear scale.*

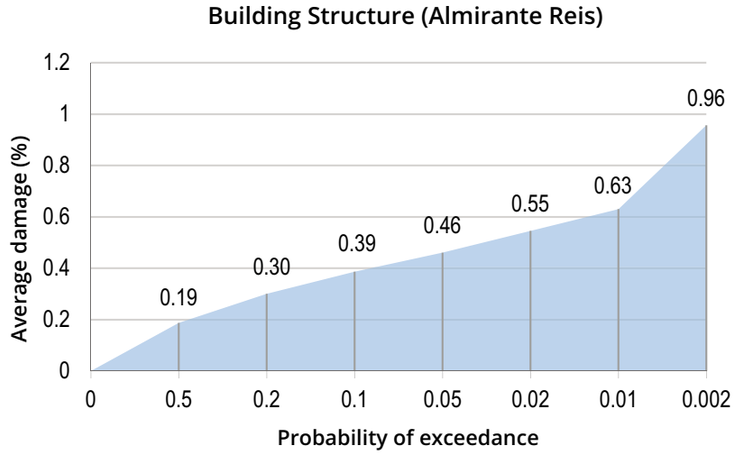

Figure 4. *Example of probability-damage curve on the structure of the buildings of the sub-basin that extends along Avenida Almirante Reis (Lisbon), obtained by linear interpolation of return periods analyzed. Source: production of the author.*

flood risk mapping

Flood risk mapping comprises the geographic representation of the flood characteristics, the exposed elements and the result of the risk assessment of those elements according to several criteria. The purpose of this cartography consists of the differentiation of the different elements taking in account if the risk of flooding is higher or lower, resulting in a fundamental tool for the management and planning of mitigation measures or to adapt to it. This cartography comprises maps of flooded areas, the susceptibility maps; the elements exposed and flood risk, among others.

maps of flooded areas

The maps of flooded areas consist of the geographical boundaries of the areas that could be affected by flooding in accordance with one or more probabilities. These are the most common maps within this theme and they may present the floods disaggregated or aggregated by different probabilities for different qualitative flood levels: i) floods with low probability (eg. return period exceeding 100 years), ii) flood with moderate probability (eg with a return period equal to or lower than 100 years and above 50 years) and iii) high probability floods (eg return period of lower than 50 years) (EXCIMAP, 2007). Although the aggregation of information in qualitative levels is better understood by the community in general, its usefulness is reduced to quantify the risk of flooding.

maps of flood risk

The cartography of risk represents the geographical boundaries of the areas where flooding may occur, disaggregated by different degrees of probability (low, medium and high or return periods) and associating information on the type of flooding, the flood extent, depth, the speed and / or direction of flow (De Moel et al., 2009). Since there are maps that may contain a great deal of information it is usual to be subdivided in maps of depth, flow and propagation floods.

map of flood depth

The maps of flood depth show the difference between the level of flooding and the land for a certain episode or probability of occurrence. The values can be derived from hydrodynamic models (2D and 3D), statistical analysis of observations made in the flooded areas (during an episode of flooding or through the marks left, for example, in buildings), surveys of the population, etc. (EXCIMAP, 2007).

map of flow and propagation of floods

The maps of flow and propagation of floods show the directions and speeds of the dominant water or a particular time of a flood. Both the necessary information and its rendering consist of very specialized job, and its implementation is particularly difficult. For these reasons there are few examples of this type of cartography (EXCIMAP, 2007).

maps of characterization of the exposed elements

It consists of cartographic representation of the elements exposed to floods and their classification and may comprise such diverse topics as the environment, heritage, infrastructure, economic or other activities relevant to the purpose of risk analysis (Schanze et al., 2006). The characterization of the exposed elements can be considered as the parameter to list the characteristics or parameters that confer vulnerability; however the absence of any reference to a higher or lower capacity of that element to resist to floods.

Given this reference or discretization we obtain maps of vulnerability to flooding (see e.g. Fekete, 2010).

flood risk map

The flood risk maps define a space for the potential adverse consequences associated with floods and these result from aggregating the losses associated to various degrees of probability of flooding. The risk can be presented in monetary value or alternatively in a percentage of damage. There are also some examples where risk is presented in a qualitative way.

Community directive n. º 2007/60/EC and the Decree-Law that makes the transposition of this Directive into Portuguese law, define that the flood risk maps should express the number of inhabitants and / or economic activities in areas potentially affected, installations that may cause pollution in case of flooding or other relevant information.

However, the identification and characterization of these elements only provide us with parameters of vulnerability (EXCIMAP, 2007), being required a further analysis to obtain flood risk cartography.

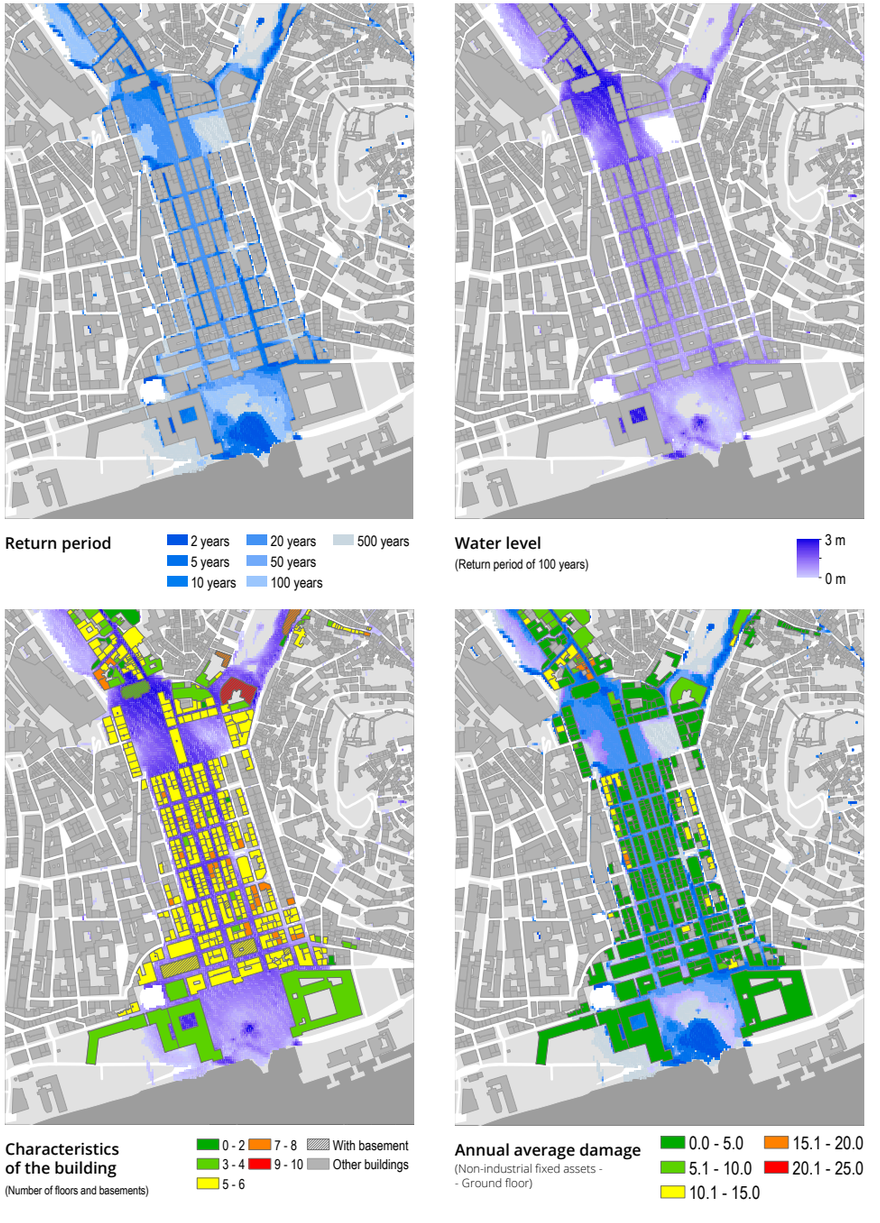

Figure 5. Different types of cartography related with floods. From left to right: Map of flooded areas, flood hazard map, Map of exposure to flooding and flood risk map. Source: production of the author using data from the Lisbon City Hall and hydrodynamic modeling.

METHODOLOGY

"You can't cross the sea merely by standing and staring at the water."

Rabindranath Tagore

This section is subdivided in three main parts, which aims to achieve an overview of the main themes for mapping flood risk. The first part introduces the main steps needed for the treatment of rainfall data with the aim of obtaining values for different return periods, and, from these, defines project rainfall graphics to be used in hydrological modeling.

The firts part is based in two fundamental documents related with statistics hidrology, being therefore recommended the reading of (see Naghettini and Pinto, 2007, Naghettini and Portela, 2011) for a further comprehension of these themes.

In the second part some considerations on hydrological modeling are carried out, in particular on the quality of needed data and the principal results to be obtained to assess the risk of flooding. It is necessary to note that this second part is only an introduction, and it is therefore necessary to use other sources to carry out the hydrological modeling.

Finally, in the third part a methodology is presented, in order to assess the flood risk in small basins.

Each of the described steps is exemplified through data related with a case study developed for a basin of the city of Lisbon, which includes the Downtown area (Baixa) and the areas of Avenida da Liberdade and Avenida Almirante Reis.

observed precipitation data

collecting and processing weather data

Obtaining rainfall data needed to obtain return periods, and flow rates required for the calibration and validation of hydrological models can be obtained free of charge through the website of the National Information System for Water Resources

Table 4. Value of annual maximum daily precipitation measured at the weather station IGIDL for hydrological years between 1961 and 2000.

hydrological year	(x_i)	hydrological year	(x_i)	hydrological year	(x_i)	hydrological year	(x_i)
1961	46.5	1971	60.2	1981	54.0	1991	26.6
1962	91.2	1972	34.9	1982	60.3	1992	59.6
1963	56.3	1973	46.4	1983	95.6	1993	73.4
1964	47.4	1974	37.0	1984	42.6	1994	55.0
1965	55.9	1975	53.8	1985	43.2	1995	44.0
1966	42.6	1976	51.5	1986	42.9	1996	53.2
1967	89.2	1977	56.6	1987	44.1	1997	92.6
1968	82.9	1978	53.7	1988	41.4	1998	57.7
1969	52.8	1979	65.7	1989	45.2	1999	78.1
1970	37.3	1980	38.5	1990	44.6	2000	53.2

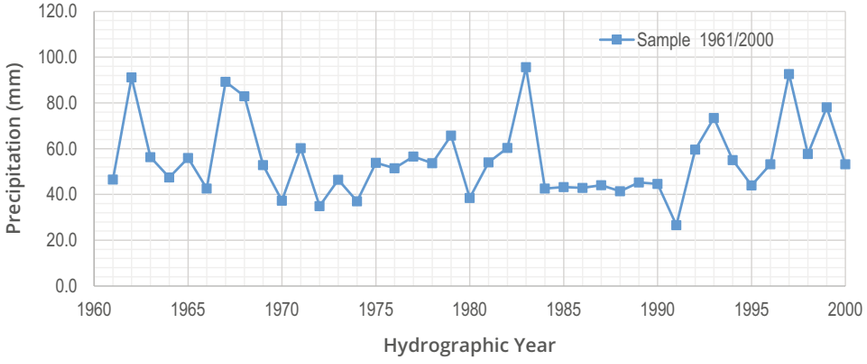

Figure 6. Maximum daily rainfall relating to hidrographic years between 1960 e 2000, (meteorological station IGIDL). Source: production of the author.

(SNIRH) [iv]. This source has data for a large number of meteorological and hydrometric stations ensuring good coverage of information for the national territory. There are other important sources that can be consulted, such as the Portuguese Institute of Ocean and Atmosphere (Instituto Português do Mar e da Atmosfera)[v].

Nevertheless, rainfall data used in this guide were obtained from the Geophysical Institute of Infante D. Luis. This institution is an integral part of the Faculty of Sciences, University of Lisbon, having at their disposal the first meteorological observatory in Portugal. The weather station is located in adjacent grounds to the building of the Polytechnic School in Lisbon.

The analysed data correspond to cumulative daily rainfall between hydrological[vi] years 1961 and 2000. The annual maximum daily precipitation values for each hydrological year (x_i) were taken from this daily sample, yielding a total of 40 values $(N = 40)$. The values of the annual maximum daily precipitation are shown in Table 4.

Some statistic analyses, designated by descriptive statistics, are used with the aim to understand the behaviour of the sample. Among these are the measures of central tendency (mean, median and mode), measures of dispersion (standard deviation and variance) and the coefficient of asymmetry.

Table 5 presents the formulas for calculation of descriptive statistics and the results obtained from the precipitation sample in Table 4. This table does not attempt to be exhaustive, exclusively presenting the statistical analyses necessary throughout this guide.

Samples in hydrology should consist of simple random variables drawn from a single population. There are, however, several situations that can influence these

iv *http://snirh.pt/ (consulted 10/2013).*

v *https://www.ipma.pt/ (consulted 10/2013).*

vi *The hydrologic year begins on 1st October (daily sample data starts on 1/10/1961 and ends 30/09/2000).*

Table 5. Main descriptive statistics, formulas and respective values obtained from the analysis of the sample presented in Table 4.

	Formula	Sample value (Table 4)[vii]
Median	$\overline{X} = \frac{1}{N}\sum_{i=1}^{N} x_i$	55.2
Variance	$S_x^2 = \frac{N}{N-1}\frac{1}{N}\sum_{i=1}^{N}\left(x_i - \overline{X}\right)^2$	281.2
Standard deviation	$S_x = \sqrt{S_x^2}$	16.8
Coefficient of asymmetry	$g_x = \frac{N^2 \frac{1}{N}\sum_{i=1}^{N}\left(x_i - \overline{X}\right)^3}{(N-1)(N-2)(S_x)^3}$	1.0301

assumptions and therefore the quality of the sample, which implies that the results obtained from its analysis are biased. To verify that same quality, assumptions of randomness, independence, homogeneity and stationarity of the sample will have to be previously evaluated. In order to verify these features there are several parametric tests, if the sample data have been obtained from a population with normal distribution or any other distribution whose model is known.[vii]

This is not the case of the sample data of extreme hydrological variables, being therefore necessary non-parametric tests. There is a multiplicity of tests that can be used for this purpose and as it is not intended to address them all, the following four tests are presented in order to evaluate each of the mentioned features.

randomness hypothesis test

The randomness hypothesis test does not allow proving that a sample is random, but proving it is not. A hydrographic sample is considered random when the variation of its values is due to natural causes. In the event that the station has changed its location, of a malfunction of the measuring system or any other event entailing changes in the measured values that are not related to natural causes, the sample is no longer random.

The randomness hypothesis can be evaluated using the nonparametric test of the number of inflections. This number of inflections (P_i) can be obtained by counting the number of "peaks" and "valleys" by observing the graphic shown in Figure 6. An excessively large or small amount of inflections means that the sample is not random.

If a sample with N elements is random, the expected value of inflections $E[p]$ is obtained by the formula provided for this parameter in Table 6, where the variance $Var[p]$ is approximated by the equation also present in this table. Theory demonstrates that the number of inflections calculated for different samples with a size superior to 30 elements follows behaviour close to a normal distribution. In this sense the statistic of the randomness test can be formulated as described in Table 6 for parameter T, being the randomness hypothesis rejected for a level of

vii *With the exception of the coefficient of asymmetry, all the values are rounded to the first decimal place.*

Table 6. Parameters required to carry out the nonparametric test of the number of inflections and respective values of test sample. In this case we can not reject the randomness hypothesis of the sample to a level of significance of 0.05 (or a confidence level of 0.95).

Parameters	Values	Parameters	Values
$N =$	40	$\lvert T\rvert =$	1.41
$E[p] = \frac{2(N-2)}{3} =$	25.33	$\alpha =$	0.05
$Var[p] = \frac{16N-29}{90} =$	6.79	$1-\alpha/2 =$	0.975
$p =$	29	$\Phi^{-1}(1-\alpha/2) =$	1.96
$T = \frac{p - E[p]}{\sqrt{Var[p]}} =$	1.41	$\lvert T\rvert > \Phi^{-1}(1-\alpha/2)$	Do not reject

significance α when $|T| > \Phi^{-1}(1-\alpha/2)$[viii]. The value of Φ^{-1} corresponds to the inverse of the cumulative probability function of the standard normal distribution (meaning with mean 0 and standard deviation 1) that can be obtained through the inverse function described in equation (9)[ix], where z is the sample value of the standard normal distribution.

$$\Phi(z) = \int_{-\infty}^{z} \frac{1}{\sqrt{2\pi}} e^{-\frac{Z^2}{2}} dz \qquad (9)$$

With the non-rejection of the randomness hypothesis of the sample it is convenient to confirm whether the elements that constitute it are independent. For this it is necessary to check that no observation of the sample influences the occurrence or non-occurrence of another value contained in the same sample. In this sense, a sample of annual maximum precipitation will have a predictably low dependence, being difficult to achieve an annual maximum influence or to be influenced by another annual maximum. There is however other reviews where this influence between events can happen, such as with the average daily flow where a value observed in a given day is often conditioned by the value of the previous day.

independence hypothesis test

There are several hypothesis tests, of which it is here presented the formulation of Wald-Wolfowitz. The statistic of this test is given by the equation of parameter R presented on Table 7, where X_i' corresponds to a given observation contained in the sample of dimension N minus the sample mean. For a set of samples with independent observations it can be demonstrated that statistic R follows the Normal distribution of the mean $E[R]$ and the variance $Var[R]$ (Table 7). This statistical test can be formulated as described in Table 7 for parameter T, which follows a normal standard distribution. Being a

viii *As it is a bilateral test we have* $(1-\alpha/2)$.

ix *The inverse function of the cumulative probability function of the standard normal distribution can be obtained for different values by consulting tables created for this purpose (see e.g. Naghettini and Pinto 2007, pp 135). There are also several computer programs that provide its calculation. As an example, Microsoft Excel provides the function INV.NORMAL(probability; media; standard_deviation). For the standard normal distribution it will be INV.NORMAL(probability;0;1).*

Table 7. Parameters required to carry out the nonparametric test of independence and correspondent values of the test sample. For this sample, and with a confidence level of 95%, we can not reject the hypothesis of independence.

Parameters	Values	Parameters	Values
$S_2 = \sum_{i=1}^{N} (X_i')^2 =$	10968.35	$\lvert T \rvert =$	0.79
$E[R] = -\frac{S_2}{N-1} =$	-281.24	$\alpha =$	0.05
$S_4 = \sum_{i=1}^{N} (X_i')^4 =$	9957732.12	$1-\alpha/2 =$	0.975
$Var[R] = \frac{S_2^2 - S_4}{N-1} + \frac{S_2^2 - S_4}{(N-1)(N-2)} - \frac{S_2^2}{(N-1)^2} =$	2818051.44	$\Phi^{-1}(1-\alpha/2) =$	1.96
$R = \sum_{i=1}^{N-1} X_i' X_{i+1}' + X_1' X_N' =$	1042.88	$\lvert T \rvert > \Phi^{-1}(1-\alpha/2)$	Do not reject
$T = \frac{R - E[R]}{\sqrt{Var[R]}} =$	0.79	—	—

bilateral test the hypothesis of independence is rejected for a level of significance α when $|T| > \Phi^{-1}(1-\alpha/2)$[x].

homogeneity hypothesis test

The following test aims to verify the hypothesis of homogeneity of the sample, that is, if all its elements are part of the same population. The identification of the presence of two populations in a given sample and more likely in long series of average values, since exceptional weather phenomena (eg El Niño) will imply significant differences in the amounts of precipitation that are not always easily detectable in the annual maximum rainfall.

To test the homogeneity hypothesis in a given sample with N elements it is necessary to split it in two subsamples, in case the value of N is even they should have the same number of elements $(N_1 = N/2)$. If N is odd, then the first subsample should have minus an element than the second one for $(N_2 = (N+1)/2; N_1 = N - N_2)$. The subsample N_1 contains the first part of the sample and N_2 the second part. After that, the sample N is ordered in ascending order and it is verified where each value of N_1 and N_2 are in the ordered serie. In case a value of N belongs to N_1 it is given value 1 to that register, if it belongs to N_2 it is given value 2. This analysis results in a column with the classification order of each value, designated by m. That is, if $m_i = 1$ then X_i is an element of N_1, if $m_i = 2$ then X_i is an element of N_2. The value of V presented in Table 8 consists of the number of times in which $m_i \neq m_{i+1}$.

The statistic of hypothesis testing is given by the parameter V, that can show that in case the samples are homogeneous, the statistics of this parameter follows a normal

x *See note vii and viii.*

Table 8. Parameters required to carry out the nonparametric test of homogeneity and correspondent values of test sample. In this case we can not reject the hypothesis of homogeneity of the sample for a confidence level of 95%.

Parameters	Values	Parameters	Values
$V =$	17	$\lvert T \rvert =$	1.28
$N =$	40	$\alpha =$	0.05
$N_1 =$	20	$1-\alpha/2 =$	0.975
$E[V] = 1 + \frac{2N_1(N-N_1)}{N} =$	21	$\Phi^{-1}(1-\alpha/2) =$	1.96
$Var[V] = \frac{2N_1(N-N_1)[2N_1(N-N_1)-N]}{N^2(N-1)} =$	9.74	$\lvert T \rvert > \Phi^{-1}(1-\alpha/2)$	Do not reject
$T = \frac{V - E[V]}{\sqrt{Var[V]}} =$	-1.28	—	—

distribution with mean equal to $E[V]$ and variance $Var[V]$, as shown in Table 8. Statistically this test can be formulated as described in the same table for parameter T, which follows a normal standard distribution. Being a bilateral test the hypothesis of homogeneity is rejected for a level of significance α when $|T| > \Phi^{-1}(1-\alpha/2)$[xi].

stationarity hypothesis test

The last test referred in this guide verifies the hypothesis of stationarity of the sample elements. A sample is not stationary when there are trends or sudden changes in their values, taking into account the chronological order of the events recorded. An example of trend may be related to variability or climate change, influencing the behaviour of precipitation and its extremes in the long term. Although this change could mean a nonstationarity of the sample, it is particularly difficult to be verified through tests of stationarity. Such phenomena are considerably long and samples typically evaluated do not have a sufficiently long period of observations for which the influence of these changes to become evident.

Abrupt variations may occur, for example, in measurements of river flow of before and after building a dam, being less common in the precipitation data, however, they may be the result of a malfunction in udometric station.

The nonparametric Spearman test is a hypothesis test for stationarity that aims to identify a possible trend in a given hydrologic sample over time. The statistic test is based on the r_s coefficient presented in Table 9 where N is the number of elements in the sample, T_t the number of the order of the element t of the sample and m_t the number of values lower or equal to the element t of the sample.

The statistics of the hypothesis test is given by r_s parameter, and it can show that if there are no correlation between the value of m_t and T_t the distribution of this parameter follows a Normal distribution with mean equal to $E[r_s] = 0$ and variance $Var[R]$, as shown in Table 9. The statistic in Spearman's test can be formulated as described in the same table for the parameter T_t, which follows a normal standard distribution. Being a bilateral

xi *See note vii and viii.*

Table 9. Parameters necessary to carry out nonparametric test of stationarity and correspondent values of test sample. In this case we can not reject the hypothesis of stationarity of the sample for a confidence level of 95%.

Parameters	Values	Parameters	Values
$r_s = 1 - \frac{6\sum_{t=1}^{N}(m_t - T_t)^2}{N^3 - N} =$	0.022	$\alpha =$	0.05
$Var[r_s] = \frac{1}{N-1} =$	0.026	$1-\alpha/2 =$	0.975
$T = \frac{r_s}{\sqrt{Var[r_s]}} =$	0.139	$\Phi^{-1}(1-\alpha/2) =$	1.96
$\lvert T \rvert =$	0.139	$\lvert T \rvert > \Phi^{-1}(1-\alpha/2)$	Do not reject

test the hypothesis of stationarity is rejected for a level of significance α when $|T| > \Phi^{-1}(1-\alpha/2)$[xii].

From the application of different hypotheses tests it appears that one can not reject the hypothesis of randomness, independence, homogeneity and stationarity of the sample elements of value of annual maximum daily precipitation observed in IGIDL weather station for the period between 1961 and 2000.

obtaining return periods

The statistical analysis for calculating return periods of annual maximum precipitation are obtained from the theory of extreme value. This theory defines the Gumbel Distribution as the most used distribution to represent the maximum, being usually designated merely by Gumbel. In addition to the Gumbel Distribution, and with the same purpose, other statistical distributions such as Pearson III, Log-Pearson III Gen, (GEV), among others, are used.

xii *Ver nota vii e viii.*

These laws consist of probabilistic models widely established in literature, and those that in theory are best suited to the most common intrinsic characteristics in samples of hydrologic variables for maximum extreme values (Naghettini and Portela, 2011).

The probability density function of Gumbel $f(x)$ is presented in equation (10).

$$f_x(x) = \frac{1}{\alpha}\exp\left[-\frac{x-\beta}{\alpha} - \exp\left(-\frac{x-\beta}{\alpha}\right)\right] \quad (10)$$

para $-\infty < x < +\infty, -\infty < \beta < +\infty, \alpha > 0$

For the purpose of adjusting the Gumbel Distribution to the sample values of annual maximum precipitation it is necessary to obtain the values of α and β, which correspond respectively, to location and scale parameters of this distribution. In Figure 7 some examples are presented in order to illustrate the behaviour of the function by different parameters. These parameters are calculated using the following equations (11), where $Var[X]$ corresponds to the sample variance, and (12) where $E[X]$ is the sample mean. In this distribution the coefficient of asymmetry is constant $(\gamma = 1.1396)$, and therefore referred to as function of two parameters.

$$Var[X] = \frac{\pi^2\alpha^2}{6} \Leftrightarrow \alpha = \sqrt{\frac{6Var[X]}{\pi^2}} \quad (11)$$

$$E[X] = \beta + 0{,}57721566\alpha \Leftrightarrow \Leftrightarrow \beta = E[X] - 0.57721566\alpha \quad (12)$$

Remember that the sample mean or the expected value $E[X]$ of annual maximum rainfall is 55.2 and its variance $Var[X]$ of 281.2. With the application of equations (11) and (12) we have α = 47.91 and β = 13.08.

The function of cumulative probabilities of Gumbel $F(x)$ is provided by the equation (13)

$$F_x(x) = \exp\left[-\exp\left(-\frac{x-\beta}{\alpha}\right)\right] \quad (13)$$

Figure 8 shows some examples of the cumulative probability function for the Gumbel Distribution and an adjustment of this law to the parameters of the sample of annual maximum rainfall. This figure also presents the values of the sample and the corresponding empirical probability of non-exceedance, calculated using the formula postulated by Weibull. This formula allows the estimation of the probability of non-exceedance, not biased for all distributions (Naghettini and Pinto, 2007).

The Weibull formula is described in equation (14) where i corresponds to the position of a particular element of the sample after sorting all its elements

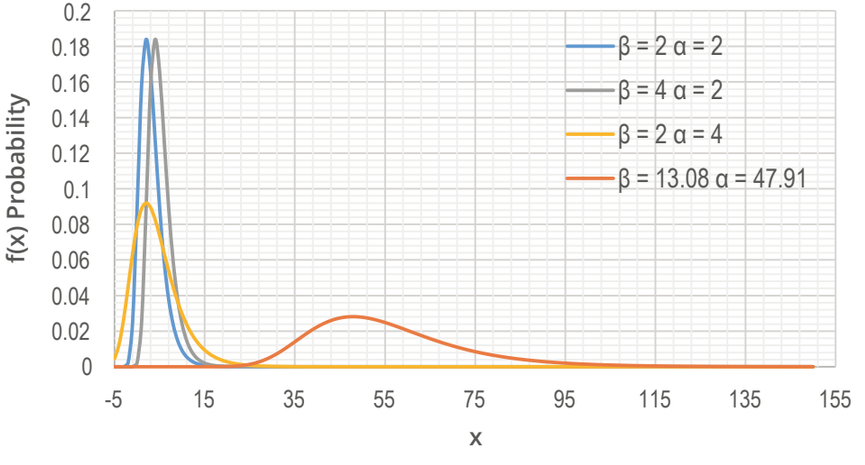

Figure 7. Example of the application of the density functions of Gumbel distribution for different scale and location parameters. The example with α = 13.08 e β = 47.91 correspond to the parameters of the sample of annual maximum rainfall (hidrological year) between 1961 and 2000 for the hydrographic station IGIDL (Lisbon). Source: production of the author.

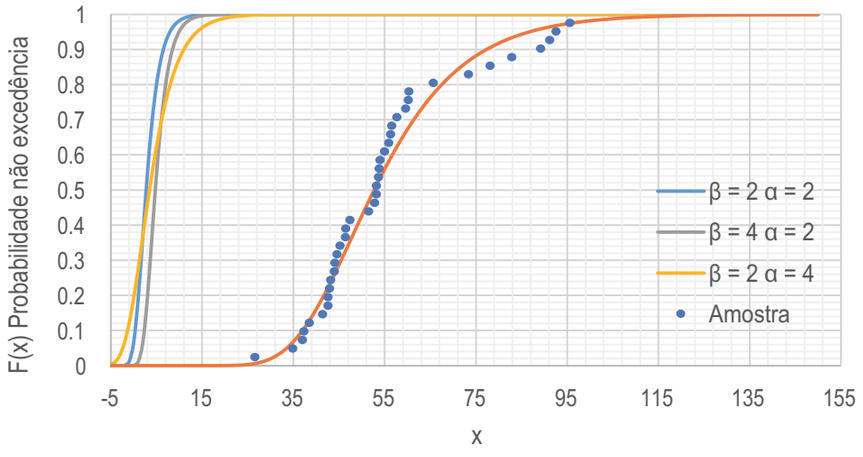

Figure 8. Example of the application of the function of cumulative probabilities of the Gumbel Distribution for the different parameters shown in Figure 18. Source: production of the author.

in ascending order and N to the sample dimension, which for the annual maximum rainfall between 1961 and 2000 is 40.

$$F = \frac{i}{N+1} \quad (14)$$

Figure 8 provides a first visual perception of the adjustment of the Gumbel Distribution to the distribution of the sample, however the correspondent graphical representation and visual assessment must be made using the role of probabilities (see Figure 9 as an example). For this law it is also important to check if the coefficient of asymmetry parameter or sample location parameter $(\gamma[X]=1.0301)$ is aproximated to the Gumbel Distribution $(\gamma=1.1396)$ which is the case. These are two indicators that can contribute to the choice of this distribution over others; however there are other criteria that may influence this choice. Any such criteria as the representation of the function in the role of probabilities will be discussed later in this guide.

Being this the chosen law, the quantiles of the distribution (equivalent to the return periods) can be obtained from equation (7), where T corresponds to the desired return period (in years).

$$x[T] = \beta - \alpha \ln\left[-\ln\left(1-\frac{1}{T}\right)\right] \quad (15)$$

As previously mentioned, there are several distributions that can be applied to the statistical calculation of return periods of annual maximum precipitation. As the aim is not to present all existing distributions, it is deemed pertinent to expose another distribution, since it is recommended to apply different distributions in the estimation of return periods, in order to pick one that best fits to the sample analysis (Naghettini and Pinto, 2007, Naghettini and Portela, 2011). In this sense, the law of Pearson III, is presented as it is the most applied in this type of studies, after Gumbel.

The probability density function of the distribuition of Pearson III $f(x)$ is presented in equation (16) where α, β and γ are respectively, the parameter of scale, shape and location. The distribution of Pearson III is a three parameteres function since, unlike the Gumbel Distribution, the location parameter is not constant.

$$f_x(x) = \frac{1}{\alpha\Gamma(\beta)}\left(\frac{x-\gamma}{\alpha}\right)^{\beta-1}\exp\left(-\frac{x-\gamma}{\alpha}\right) \quad (16)$$

para $\gamma < x < \infty$

Parameters α, β and γ are estimated through equations (17), (18) and (19), where $\gamma[X]$ is asymetry coeficient of the sample, $Var[X]$ its variance and $E[X]$ its mean.

$$\gamma[X] = \frac{2}{\sqrt{\beta}} \Leftrightarrow \beta = \left(\frac{2}{\gamma[X]}\right)^2 \quad (17)$$

$$Var[X] = \alpha^2\beta \Leftrightarrow \alpha = \sqrt{\frac{Var[X]}{\beta}} \quad (18)$$

$$E[X] = \alpha\beta + \gamma \Leftrightarrow \gamma = \frac{E[X]}{\alpha\beta} \quad (19)$$

The function of cumulative probabilities of Pearson's III distribution $F(x)$ is calculated using equation (20).

$$f_x(x) = \frac{1}{\alpha\Gamma(\beta)}\int_{\gamma}^{\infty}\left(\frac{x-\gamma}{\alpha}\right)^{\beta-1}\exp\left(-\frac{x-\gamma}{\alpha}\right)dx \quad (20)$$

For Pearson's III distribution there is no simple analytical way that allows the calculation of quantiles (Naghettini and Portela, 2011). Since this is the necessary information to obtain the corresponding rainfall associated with a given return period, there are other approaches that simplify the calculation. This approach is available for distribution Pearson III, as well as other distributions through the use of probability quantile for calculating factors, which has been introduced by Chow (1954).

In this method the quantiles are obtained from equation (21), where x_F corresponds to the quantile probability of no exceedance F being equal to a determined return period $\overline{X}$ which correspond to the sample distribution's mean and S_X to its standard deviation. The value of K^F_{DIST} is obtained by calculating the expression of the probability factor of a particular distribution.

$$x_F = \overline{X} + K^F_{Dist} s_X \quad (21)$$

Equations (22) and (23) allow to calculate the probability factors for the Gumbel Distribution and of Pearson III respectively. The value of g_x, equation (23) refers to the asymmetry coefficient of the sample.

$$K^F_{Gumbel} \cong -\frac{\sqrt{6}}{\pi}\left\{0.57721566 + \ln\left[\ln\left(1-\frac{1}{T}\right)\right]\right\} \quad (22)$$

$$K^F_{Pearson} = K^F_{Normal} + \left(K^F_{Normal}{}^2 - 1\right)k + \\ + \frac{1}{3}\left(K^F_{Normal}{}^3 - 6K^T_{Normal}\right)k^2 - \\ -(K^F_{Normal}{}^2 - 1)k^3 + K^F_{Normal}k^4 + \\ + \frac{1}{3}k^5 \text{ sendo } k = \frac{g_x}{6} \quad (23)$$

Table 10. Results obtained through the use of the probability factors of the distribution of Gumbel and Pearson III of different quantiles.

T	$1-\frac{1}{T}$	K^F_{Gumbel}	x_f (Gumbel)	K^F_{Normal}	$K^F_{Pearson}$	x_f (Pearson III)
2	0.500	-0.164	52.44	0	-0.167	52.40
5	0.800	0.719	67.26	0.842	0.750	67.77
10	0.900	1.305	77.07	1.282	1.335	77.58
20	0.950	1.866	86.48	1.645	1.877	86.57
50	0.980	2.592	98.67	2.054	2.556	98.05
100	0.990	3.137	107.80	2.326	3.050	106.34
500	0.998	4.395	128.89	2.878	4.159	124.94

To calculate the probability of the law Pearson III factors it is necessary to obtain the factors of probability of the normal law. These correspond to the inverse function of the cumulative probability of the normal standard distribution, which can be obtained through the inverse function described in equation (9)[xiii].

As previously mentioned, one of several criteria for the choice of a particular law over other consist of the visualization of the distributions on probability graphic. These graphics have in the ordinates axis grading and values in the sampling units and in the abscissa axis a transformed probability scale. Thus, the empirical probabilities of non exceedance have to be allocated to the values of the sample, as there are several formulas that allow this assignment with different levels of adequacy for different objectives (see Naghettini and Portela, 2011).

In this particular case the aim is to check the visual setting of Pearson III and Gumbel distribution to the sample of extreme values. Accordingly, and for the assignment of empirical probability of non exceedance to the sample, it was used the Weibull formula since it has the attributes not to bias the probabilities of non exceedance for all distributions. The application of this formula was shown previously to be the procedure adopted for viewing the sample in a probability graphic, identical to the described in Figure 8.

To assign a scale of probabilities to the abscissa linear scale it is necessary to consider what you want to withdraw from the observation chart, since there are different probability roles as those that refer to Normal distribution or the Gumbel distribution.

A visual comparison of two distributions (Gumbel and Pearson III) and the correspondent adherence to the sample is preferably performed using the role of the Probabilities of the Normal law. Meanwhile, when comparing a sample with a single distribution of extreme, it should be used the role of probabilities of that distribution. This situation usually occurs when you already have knowledge of the law of extremes which best fits to the sample (Naghettini and Portela, 2011).

Figure 9 presents sample data after ascending order and the attribution of the empirical probability of non exceedance

xiii *See note viii*

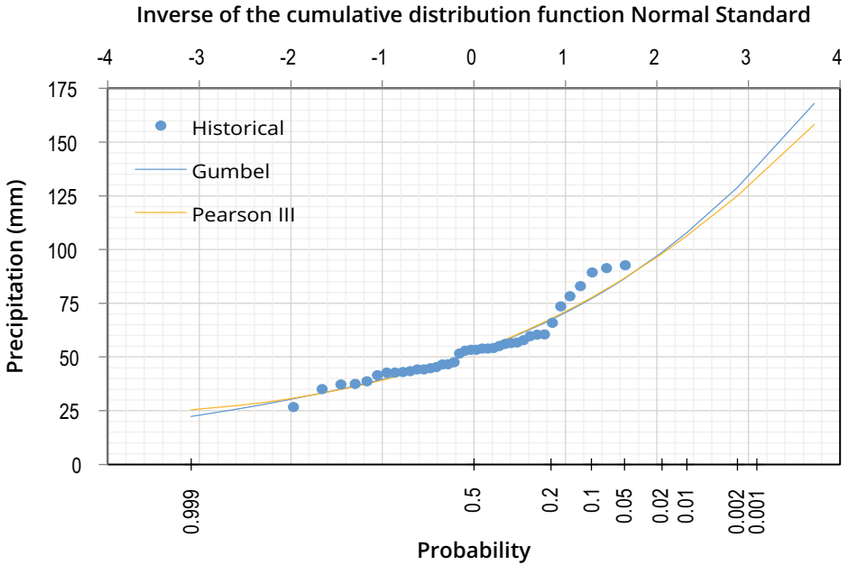

Figure 9. Ajustment of the Gumbel Distribution (Extreme values type I) and Pearson III to the annual maximum sample of observed precipitation between 1961 and 2000. Source: production of the author.

formulated by Weibull, as well as the result of the adjustment to the sample of the Gumbel Distribution and Pearson III. From its observation it can be concluded that both distributions have a similar behaviour and identical adjustment to the sample.

When distributions have identical adjustments to the sample, you should choose the one with fewer parameters. As mentioned distribution of Pearson III consists of a model with three parameters, which its application provides results with more flexibility and therefore a greater adherence to the sample. However, this adherence is achieved at the expense of the third parameter which is obtained from the sample, which increases the uncertainty of the estimated values (see Figure 10). On the other hand, the Gumbel distribution is adjusted while maintaining the location parameter (or coefficient of asymmetry) of its constant distribution, which is equal to 1.1396. This parameter has a value of 1.0301 in the sample, both being very similar. When this situation arises we have another argument for choosing the Gumbel Distribution regarding other distributions.

There are however, a number of tests of adherence of statistical laws to the sample, as for example, the chi-square, Kolmogorov-Smirnov, Anderson-Darling or Filiben. These tests generally present deficiencies in obtaining the differences between the frequency distributions of the laws of extremes and the sample in the upper and lower tails (Naghettini and Pinto, 2007). In the analysed situation of the annual maximum rainfall values, the differences in the

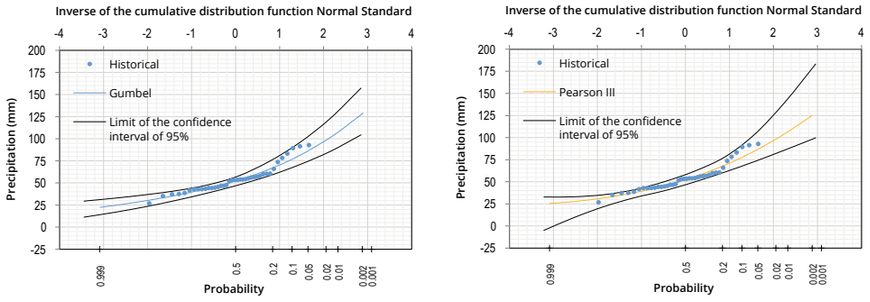

Figure 10. Result of applying the Monte Carlo method for obtaining confidence intervals in estimated values by the application of the Gumbel Distribution (left) and Pearson III (right). This figure shows the greatest amount of uncertainty associated with a distribution of three parameters in comparison with another two. Source: production of the author.

upper tails are the most important since they correspond to the values of the higher return periods. This situation makes the adherence tests currently available, limited to this purpose (Naghettini and Portela, 2011). For this reason its application was not taken into account in the choice of the statistical law which best fit to the distribution of the sample[xiv].

The application of statistical laws of extreme values and the consequent attainment of quantile contains a certain level of uncertainty regardless of the method applied. This uncertainty is present from the beginning of the analysis, obtaining the necessary parameters for a distribution from a sample. The sample of annual maximum daily precipitation only contains a small number of observations, so it is not possible an accurate characterization of its entire population, as it is infinite.

However this uncertainty can be estimated using different methods, as for example the Monte Carlo method. This method consists of the generation of several series (never less than 5000) of random numbers between 0 and 1 with the same sample size. Then, for each of the random series generated, the distribution that was initially used to calculate the return periods is adjusted, providing probability factors of that distribution for each value of each series (for the Gumbel Distribution equation (22) is applied and for the Pearson's III equation (23)).

With the application of equation (21) to the probability factors, random values series are obtained of precipitation adjusted to the distribution. Finally, for each of these series, desired quantile of precipitation (equivalent to the return periods) are obtained and the estimation of confidence intervals made. That is, to a level of significance of 0.05 (or confidence interval of 95%) are chosen the random series generated that correspond to the 2.5% percentile for the lower limit of the confidence interval and the percentile 97.5% for the upper (see Table 11).[xv]

xiv *In order to obtain further information about the adherence tests consult Naghettini and Pinto (2007), pages 270 - 286.*

xv *Taking in account the extent of the analysis required for the calculation of uncertainty using the Monte Carlo method, there are several software that incorporate its algorithm. The confidence intervals shown in Figure 10 and quantified in Table 11 were obtained using the program Hydrognomon (available on http://hydrognomon.org/)*

Table 11. Values of return periods obtained with the application of the Gumbel Distribution and Pearson III and correspondent lower and upper values of the confidence interval of 95% resulting from the application of the Monte Carlo method. In this table, it can be verified a greater range between the lower and upper limits of the confidence interval resulting from the application of the law of Pearson III compared with the Gumbel Distribution.

	Return period	2	5	10	20	50	100	500
	Probability of non exceedance	0.5	0.8	0.9	0.95	0.98	0.99	0.998
Gumbel	Lower value of the confidence interval 95% (mm)	46.9	59.7	67.7	75.0	83.8	90.6	104.3
	Adjustment of the Gumbel Distribution Maximum (mm)	52.4	67.3	77.1	86.7	98.7	107.8	128.9
	Upper value of the confidence interval 95% (mm)	57.0	77.1	90.6	103.6	119.6	132.2	157.3
Pearson III	Lower confidence interval 95% (mm)	46.8	60.1	67.8	74.2	82.0	87.2	98.1
	Adjustment of the Law of Pearson III (mm)	52.4	67.8	77.6	86.5	98.0	106.3	124.9
	Upper confidence interval 95% (mm)	58.5	76.9	92.7	107.4	129.1	144.1	178.2

From the different analyzes presented, it may be concluded that the most appropriate law to obtain return periods based on the values of annual maximum rainfall of the sample shown in Table 4, is the Gumbel Distribution, being its values used to obtain the hyetographs.

definition of hyetographs

Hyetographs result from the need to distribute the dailly precipitation in shorter periods of time, with the purpose of creating a hydrological modelation of a determined hydrographic basin. Depending on the dimension of that basin and of the capacity of the hydrological model, hyetographs can be drawn for a precipitation with higher or lower duration and subdivided in shorter or longer periods of time or time blocks.

The choice of the length of the hyetographs has subjacent the processing time of the hydrological model (the longer the duration of the hyetographs the larger the processing time) and the concentration period of the basin, that is the period of time the precipitated water traveled between the most distant end and a certain section of the water line (Martins, 2000). So, reached the maximum precipitation of the hyetograph, its remaining duration must be greater than or equal to the concentration time of the basin, so as to ensure that the maximum peak of precipitation affecting the top of the basin reaches its end, thus ensuring that the maximum extent of the flood is modeled.

The choice of time blocks of the hyetograph takes into account the phenomenon that is intended to model, more widely spaced in the case of progressive flooding and basins with large dimensions; or shorter in the modeling of small and medium size basins hit by flash floods.

Table 12. Necessary data and concentration time calculation, result of the basin under study, according to the formula of Temez.

L_b (Km)	Z_{max} (m)	Z_{min} (m)	i_m (m/m)	t_c (h)
4.81	80.42	4.24	0.07	1.63

The river basin taken as an example, develops from downtown Lisbon north through the Avenida da Liberdade and Almirante Reis, may be considered a small bowl, usually plagued by flash floods. In this respect the time of hyetographs should be as small as possible.

There are several formulations for obtaining the concentration time for a given basin. Since for the case discussed here, it is only necessary, an approximation of the value of the concentration time, a single example is presented in equation (24), according to the formula proposed by Temez (1978), where t_c is the concentration time in hours, L_{bk} the length of the main water course of the basin in kilometers and i_m the average slope of the main water course of the basin. The parameter i_m can be obtained through the quota difference between the extremety upstream (Z_{max}) and downstream (Z_{min}) of the main water course on its length in meters (L_{bm}).

$$t_c = 0.3\left(\frac{L_{bk}}{i_m^{0.25}}\right)^{0.76} \quad \text{sendo } i_m = \frac{Z_{max} - Z_{min}}{L_{bm}} \qquad (24)$$

Obtaining the length and data needed to calculate the slope of the main water line can be the result from different procedures, which includes the in situ measurement. However, the fact of the river basin under study, being strongly artificialized raises some challenges, since different waterways that compose it are channeled as part of the drainage system of Lisbon city itself. As we only want to get a sense of the value of the concentration time, it can be used a digital terrain model to delineate these theoretical watercourses and from these select the one that has the greatest range corresponding to the main water course[xvi].

The concentration time of the basin obtained by the formula of Temez corresponds to the time required for the water to traverse across the basin in case this is in a state close to natural. Bearing in mind that the basin under study is composed of impermeable soils and artificial drainage systems, concentration time will be much lower. However, this analysis allows to decide the length of the hyetograph taking into account the type of modeling to be achieved.

Taking into account the concentration time and the type of flooding that occurs in this basin, we chose hyetographs lasting 4 hours divided into alternating blocks of 5 minutes.

The hyetographs associated with precipitation with different return periods are normally obtained by using a curve Intensity-Duration-Frequency (IDF), which was already mentioned, that have been defined by Brandão et al. (2001) for various weather stations of the national territory, taking into account the breaks of the evolution of the intensity of precipitation identified by those authors. Consequently, the IDF curve for a given return period is constituted by three sections, the first valid between 5 and 30 minutes, the second between 30 minutes and 6 hours, and the third between 6 and 48 hours (see Table 2).

xvi *This operation is easily carried out through a geographic information system.*

For some stations discontinuities in the transitions are identified between these consecutive sections due to their distinct expressions. When constructing hyetographs, with small time increments, based on excerpts from the IDF curve, precipitation blocks with negative values can arise, relative to meteorological stations where these discontinuities are identified. If this situation occurs, it is usually used for this time step, the section of the IDF curve immediately before the appearance of this discontinuity (Portela et al., 2000).

Data relative to IDF curves defined by Brandão et al (2001) for the udometric post of IGIDL in Lisbon has a discontinuity between the second (30 minutes to 6 hours) and the third section (6 to 24 hours) in these curves, when applied to blocks of hyetographs with duration of 5 minutes. However, since the length of the hyetographs to define is composed of 4 hours duration, this discontinuity is not relevant to the calculations performed.

The division into blocks required to achieve the precipitation hyetographs associated with a given return period can be obtained by applying equation (6) using the parameters a and b given in Table 2.

Table 13 synthetizes the necessary procedures to obtain a hyetograph with blocks of 5 minutes decreasing precipitation, for an event lasting four hours and a return period of 10 years $\left(P(5\,\text{min})_{(T10)mm}\right)$. Total precipitation for this return period is 77.1 mm and was obtained from the sample values of annual maximum daily precipitation using the Gumbel Distribution (Table 11).

The procedures illustrated in this table consist of applying the parameters of the IDF curve of IGIDL station to obtain the intensity of precipitation in millimeters per hour for each 5 minute period ($I_{(mm/h)}$ – 6th column of the table), followed by the multiplication of this intensity by the duration in hours corresponding to the time step i, to obtain their correspondent accumulated precipitation ($P(D)_{mm}$ – 7th column of the table). The following calculation aims to adjust the precipitation calculated in the previous step. This need derives from the differential between the intensity of precipitation for the period of 24 hours, associated with the return period of 10 years which was the basis of the calculation of IDF curves and the value obtained for the same conditions using the sample that supports this guide (77.1 mm).

To this end and after determining the precipitation associated with the IDF curve for a duration of 24 hours (corresponds to the last line of the 6th column of Table 13 - 78.5 mm), we calculate the ratio between these two values. Multiplying this ratio by the values of $P(D)_{mm}$ results in the accumulated precipitation adjusted to this sample ($P(D)_{(T10)mm}$ – 8th column of the table). Finally, the values to be used in the construction of the hyetograph results from the calculation of 5 minutes blocks of precipitation ($\left(P(5\,\text{min})_{(T10)mm}\right)$ – last column of the table) through the difference between adjusted

accumulated precipitation of two consecutive durations ($P(D)_{(T10)mm_i} - P(D)_{(T10)mm_{i-1}}$ to $i > 1$). The only exception concerns the first block where the value is equal to the correspondent adjusted cumulative precipitation ($P(D)_{(T10)mm}$ to $i = 1$).

The hyetograph that directly results in Table 13 consists of, and as mentioned above, a hyetograph of blocks of 5 decreasing minutes, that is, the value with higher precipitation is assigned to the first time block, decreasing this value up to 4 hours. There is however a slight increase in precipitation in the first (5 to 30 minutes) to the second section (30 minutes to 6 hours) of the IDF curve in the depicted return period. This holds for all transitions between IDF curves of IGIDL station.

The hyetograph of alternating blocks only differs of the one of descending blocks in

Table 13. Application of the IDF curve on the return period of 10 years defined for the IGIDL station in Lisbon, the return period of 10 years of precipitation (77.1 mm) obtained by adjusting the Gumbel Distribution (Table 11) to the values sample of annual maximum daily precipitation (Table 4).

i	$D_{(\min)}$	$D_{(h)}$	a	b	$I_{(mm/h)} = aD_{(\min)}^{\ b}$	$P(D)_{mm} = D_{(h)}I_{(mm/h)}$	$P(D)_{(T10)mm} = \frac{77.1}{78.5} \times P(D)_{mm}$	$P(5\min)_{(T10)mm}$
1	5	0.08	239.69	-0.486	109.64	9.14	8.97	8.97
2	10	0.17	239.69	-0.486	78.28	13.05	12.81	3.84
3	15	0.25	239.69	-0.486	64.28	16.07	15.78	2.97
4	20	0.33	239.69	-0.486	55.89	18.63	18.30	2.52
5	25	0.42	239.69	-0.486	50.14	20.89	20.52	2.22
6	30	0.50	407.36	-0.637	46.67	23.34	22.94	2.40
...	...	...	...	...	...	...	...	...
48	240	4.00	407.36	-0.637	12.41	49.64	48.75	0.37
—	1440	24.00	670.81	-0.732	3.27	78.50	77.10	—

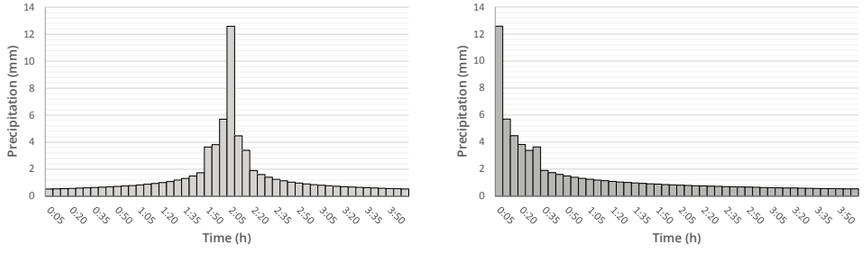

Figure 11. Hyetograph of alternating blocks (left) and decreasing blocks (right) obtained through the application of the IDF curve for the return period of 100 years, adjusted to the precipitation obtained for the same return period, through the application of the Gumbel distribution to the sample of annual maximum daily precipitation of the IGIDL weather station - Lisbon. Source: production of the author.

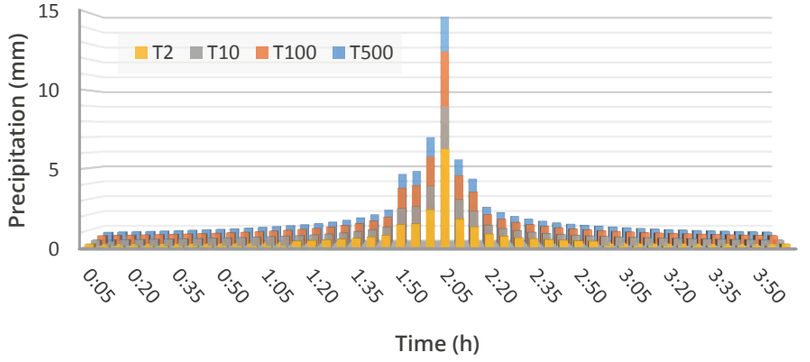

Figure 12. Hyetographs of alternating blocks for return periods of 2, 10, 100 and 500 years obtained through the application of the IDF curve for the correspondent return period, adjusted to the precipitation obtained for the same, through the application of Gumbel distribution to the sample of annual maximum daily precipitation of the IGIDL weather station - Lisbon. Source: production of the author.

the ordering of values. In this, the highest--precipitation value is centered on the distribution and the remaining values of the decreasing blocks are allocated alternately to the right and left of this central value (Figure 11).

Figure 12 illustrates some of the hyetographs used in the hydrologic modeling for the hidrographic basin under study. This figure does not present the hyetographs for the return period of 5, 20 and 50 years also used for modeling.

hydrological modeling

The assessment of flood risk encompasses the execution of several tasks. The first of which is to produce scientific data that characterizes the flood that a determined system is exposed to. This characterization consists in the definition of return periods and defining project hyetographs, taking into account the characteristics of the study area. All of these procedures have as fundamental aim the spatial flood, using to this end, models that allow to simulate the behaviour of the precipitated water in a given physical space. The Mohid[xvii] model adopted in this guide, allows modeling the runoff and main city network drainage, corresponding to a 2D model, in spite of incorporating some components of a 3D model like the simulation of network drainage. This kind of models are the most suitable for the type of basin under study where soil permeability is quite low and the worst type of flood are flash floods (see e.g. De Moel et al., 2009, Ernst et al., 2010, EXCIMAP, 2007).

This model allows to obtain important data, for the creation of risk maps, as the level, direction and speed of water, as well as the extent of the flood.

xvii *This model can be obtained in http://www.actionmodulers.pt/*

Below some considerations are held to take into account in the hydrodynamic modeling process including the importance of the information details used in this process and its implications for the results. It should be noted that the hydrodynamic modeling itself and its processes are not discussed exhaustively in this document.

necessary information

There are basically three groups of information needed for the simulation of flooding using the hydrodynamic modeling.

The first consists of a digital terrain model (DTM) and, depending on the basin under study, the geographical data of the artificial drainage network.

For the production of microscale flood risk maps it should be odopted a MDT with a horizontal resolution between a meter and 10 meters and a vertical resolution of no less than 0.5 meters (Ernst et al., 2010). These features allow us to identify small changes in the terrain, being a key factor for a correct modeling of floods. No less important is the inclusion in this digital terrain model of barriers to the flow of water, including the buildings in the basin. Nevertheless, the level of detail of the MDT can be changed if constructed with a lower level of detail and resolution with the aim of reducing the analysis time. The higher the resolution of the MDT greater the number of iterations performed by hydrodynamic models to achieve the desired results.

The drainage network has a key role when the basin is located in very artificial areas, and it should achieve a compromise between the detail of the network used and the modeling capacity. Again, the greater detail the drainage network has, the higher the model processing time, and may even make it unstable.

Information sources for this first group of information consists primarily on data obtained from the municipal services (surveying and artificial drainage systems) or surveys conducted by government institutions (topography)[xviii]. However, depending on the location and the desired detail it can be necessary to make up their own surveying using, for example, Lidar[xix] (*Laser Detection and Ranging*). It remains to note that obtaining the correct characterization of the artificial drainage systems (height and location of collectors, perimeter and shape of ducts, etc..) is especially difficult, since they refer to structures which are in operation for many years and the practice of their survey and systematic characterization has not always been implemented.

The second group of data to obtain corresponds to land use and soil occupation. This collection of information is aimed to characterize the different elements of the basin and the assignment of multiple criteria for both waterproofing and roughness, in order to simulate as accurately as possible the behaviour of water in the basin under study. Typically European organizations recommend the use of *Corine Land Cover*[xx] (minimum unit mapped of 25 acres), though there are other sources with more detailed information such as the Maps of

xviii *As example the Portuguese Geographic Institute and the Army Geographic Institute*

xix *This technique consists of an Airborne Laser system, which makes the direct measurement of elevations.*

xx *http://www.eea.europa.eu/data-and-maps/data/corine-land-cover-2006-raster(consultado 10/2013).*

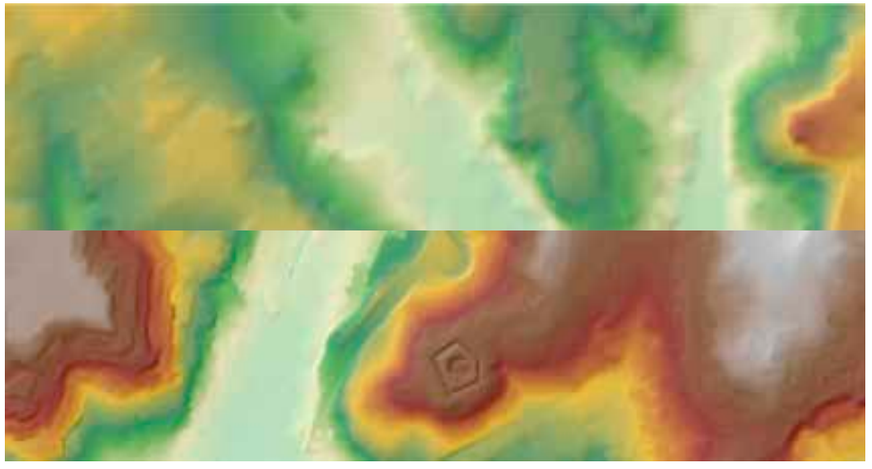

Figure 13. *Digital terrain model with vertical resolution of 0.001 meters and horizontal spatial resolution of 10 meters – upper image (central area of the city of Lisbon) and 5 meters – lower image (zona de Algés). production of the author using data from the Municipality of Lisbon, Oeiras City Council and Municipia IM, SA*

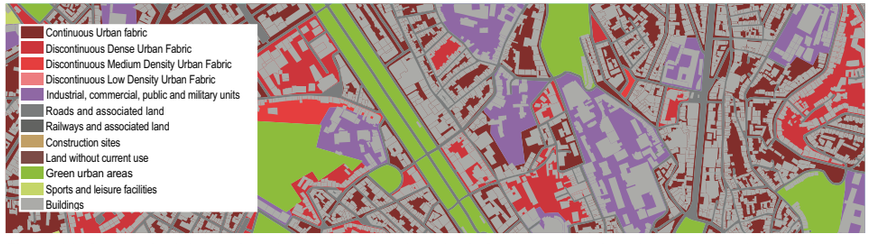

Figure 14. *Charts with information of use and occupation of soil. Source: production of the author using data from the Municipality of Lisbon and the European Environment Agency.*[xxii]

Soil Occupancy[xxi] (COS2007 - minimum unit mapped of 1 acre), the photointerpretation, municipal mapping, among others (see eg Bruijn et al., 2009 Julian et al., 2009).

The third and final group of data corresponds to historical information, with information of great importance both for the purposes of calibration and validation of hydrodynamic models. The information to be collected include: flood maps previously executed; historical records of flow levels; historical records and previous work on the speed of runoff and flood marks (eg on buildings or other structures); collection of flood events through secondary sources (eg news from newspapers), use of aerial photographs and satellite images, since

xxi *http://www.igeo.pt/produtos/CEGIG/Cos2007.htm (consulted 10/2013).*

xxii *http://www.eea.europa.eu/data-and-maps/data/urban-atlas (consulted 10/2013).*

remote sensing can bring relevant information to validate models by comparing the obtained results by the hydrodynamic modeling of a particular event and the image obtained of that same event (EXCIMAP, 2007).

results to be obtained

The hydrodynamic models are advised for flood modeling, and aims to produce risk maps. These allow obtaining a particular episode of flooding, floodplains, flood depth (as a result of the difference between the flood level and terrain) and the distribution of the velocity and direction of flow (if you use 2D models). This episode will have associated a certain probability of occurrence, which is reflected in its return period. The combination of one or more elements that characterize the flood with the occurrence probability that allows us to obtain flood risk maps (EXCIMAP, 2007)

Figure 15 illustrates some of the results obtained after modelling the floos for the hydrographic basin under study. This modeling is created based on a grid with spatial resolution of 4 meters, which takes into account the existing buildings along the basin. It was calculated the maximum water levels of precipitation associated with the respective occurrence probability for all return periods considered and grid points.

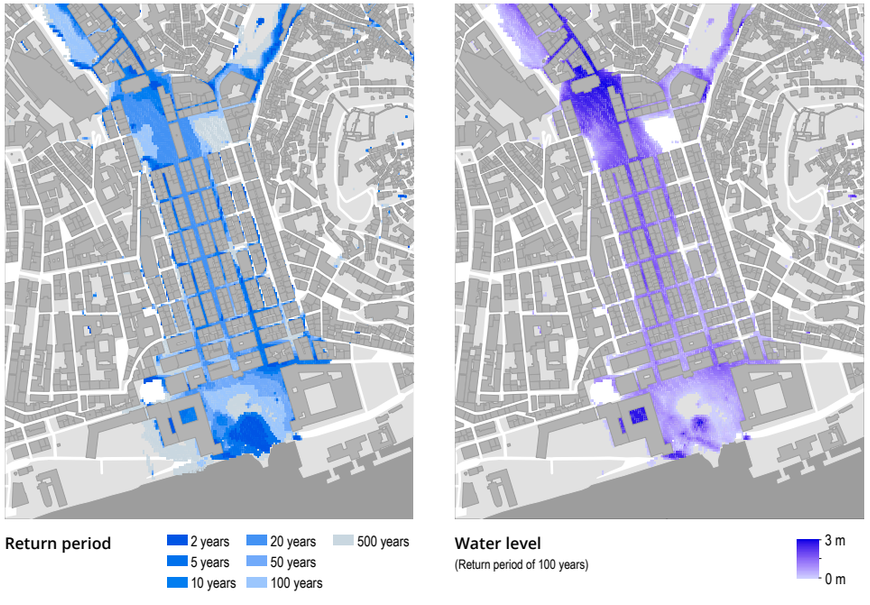

Figure 15. Maps of flood risk of downtown Lisbon basin - Avenida Almirante Reis – Avenida da Liberdade. Left – flood extension associated with different probabilities (return periods). Right - level of flood for the return period of 100 years. Source: production of the author using data from the Lisbon City Hall and hydrodynamic modeling.

flood risk assessment and cartography production

After the characterization of floods of the area under study, it begins the risk assessment process, being necessary obtaining and processing several informations. These can be defined in three large groups, consisting of i) the characterization of the elements present in the floodplains, ii) in the definition of criteria that relate to the characteristics of the flood damage in exposed elements and iii) quantifying the risk for these elements. These data will have a greater or lower detail depending on the scope of the analysis, that is, whether

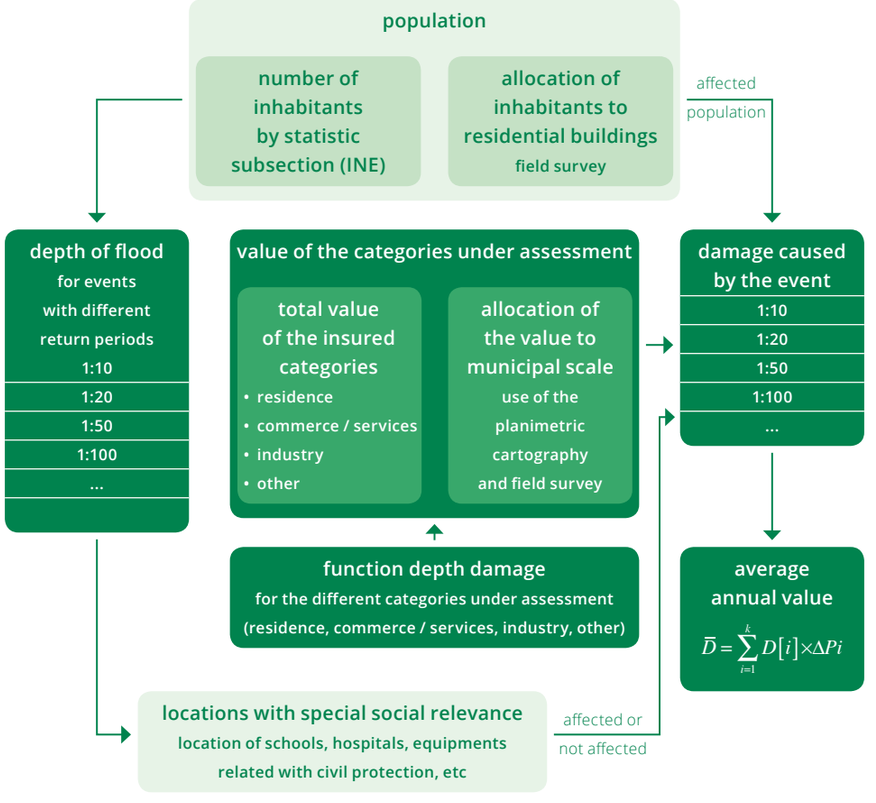

Figure 16. Methodological procedure scheme for socio-economic assessment of flood risk considering the population, economic value of the exposed elements and most vulnerable equipment in case of flooding. The blue highlights the procedure discussed in this guide. Source: adapted from Meyer et al. (2009c).

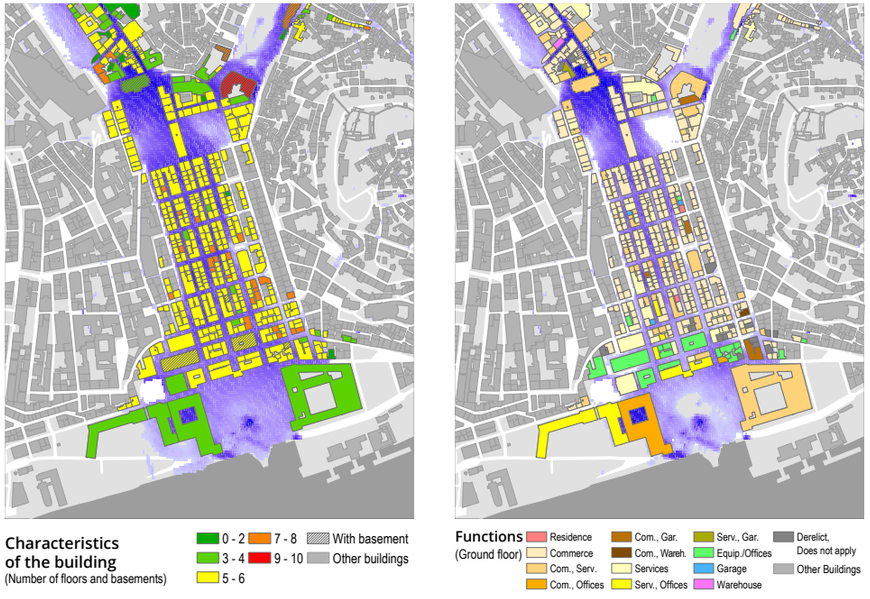

Figure 17. Maps of exposed elements. Number of floors (left) and functions of the buildings on the ground floor (right), exposed to a flood with a return period of 500 years. Source: production of the author using data from the Lisbon City Hall and hydrodynamic modeling.

the territory to assess consists of a large river basin (eg the river Tagus) then the detail of the exposed elements translated in soil occupation will be lower than in a small basin (EXCIMAP, 2007).

Also, the criteria for assessment of risk may be more or less detailed depending on the purpose of the analysis. These may include social, environmental, economic and other factors (Meyer et al., 2009c) presented in Figure 16 in schematic form. This scheme highlights in blue the procedure explored in this guide, which corresponds to the assessment risk for different categories of buildings.

necessary information

After performing all the procedures for obtaining the floodplains associated with different return periods[xxiii], it is necessary to do a survey of the exposed elements. European organizations suggest more or less directly the use of *Corine Land Cover* for this purpose (EXCIMAP, 2007). Being a cartography held to the same standard for all member states of the European Union, its use is recommended for the risk assessment in transnational and large basins. However if the scale of analysis consists of a basin of small dimension this chart is insufficient because it only offers

xxiii *As described in section Hydrological Modeling*

Table 14. Gathered elements of characterization and occupation of different buildings exposed in the basin under study. Elements related to the occupation of the building were collected for both the ground floor and to the basement. This survey is necessarily georeferenced and stored in a GIS.

Characteristics of the building	Occupation (Ground floor and Basement)	
Number of floors	Residential	Comerce
Existence of basement	Services	Equipments/Offices
Derelict	Warehouse	Garage

information about elements with an area higher or equal to 25 hectares.

In this sense it is necessary to resort to other sources or even perform a survey of the exposed elements. This is the case of the example that illustrates this guide, which seeks to assess the risk associated with each building, based on a series of damage curves, built for different uses and buildings characteristics. In this sense the need for more detailed information on the elements exposed, including the number of floors of each building and the functions located on the ground floor and basement. The decision on the number of elements to characterize this survey takes into account two criteria. The first concerns the extent of flooding for the period of highest return. In other words, it is reasonable to proceed only to the survey of the elements that are actually affected by the floods (Merz et al., 2007 Schanze et al., 2006, Meyer et al., 2009c). The second refers to the criteria that are intended to be assessed. Taking into account the damage categories illustrated in Figure 3, the elements to be surveyed should contain the necessary detail for the application of each of the damage curves presented in the same figure.

Figure 17 presents two examples of the results of a survey conducted to evaluate the basin as a result of the evidence gathered for this assessment (Table 14).

It is important to stress that these are the necessary elements for the assessment of flood risk in this particular case, having to adapt the characterization of the elements exposed to the context in which the evaluation is intended to be conducted.

obtaining and applying damage curves

The damage curves relate a particular feature of the flood with the damage (in monetary units or percentages) in a given exposed element. Since the characteristics of the exposed elements vary considerably from region to region it is appropriate to proceed to the construction of these curves using the historical data of flood damage in the area under study (see eg Bruijn et al., 2009 Meyer et al., 2009c, Wünsch et al., 2009 Messner and Meyer, 2005). There are however other possibilities to define these curves like expert consultation, resistance testing in civil engineering laboratories or surveys to the affected population (Dutta et al., 2003).

The existing literature on the definition and application of damage curves refers to its use in different contexts and purposes, in particular for i) the ratio of the speed and depth of water necessary for a person to be dragged (eg Jonkman et al, 2008); ii) damage in motor vehicles (eg Xia et al,

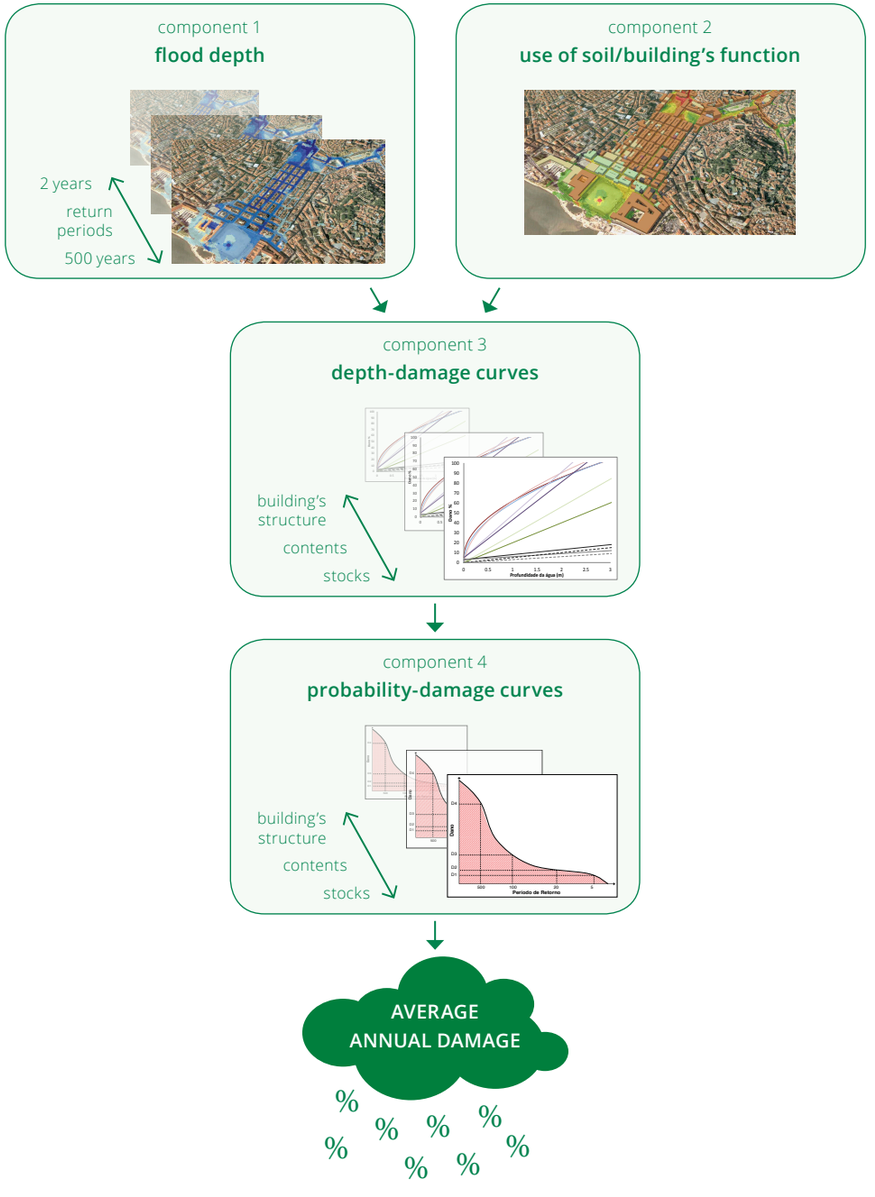

Figure 18. Methodological scheme for the evaluation of flood risk using the depth-damage curves. Source: Adapted from De Moel and Aerts (2010).

2011); iii) damage in agricultural, herding, road and railway infrastructure areas (eg De Moel and Aerts 2010), iv) damage to buildings with different levels of disaggregation (eg Wünsch et al, 2009); v) curves created for different dimensions of industry and commerce (eg Ming - Daw Su et al., 2009), among others . There are also examples in the literature where the classification of the characteristics of floods and the damage caused by these are made systematically for more than 60 years (see eg Dutta et al., 2003, Merz et al., 2004), or also deffining synthetic curves obtained by experts (see eg Veerbeek and Zevenbergen, 2009).

At present there are no databases with sufficiently systematized information

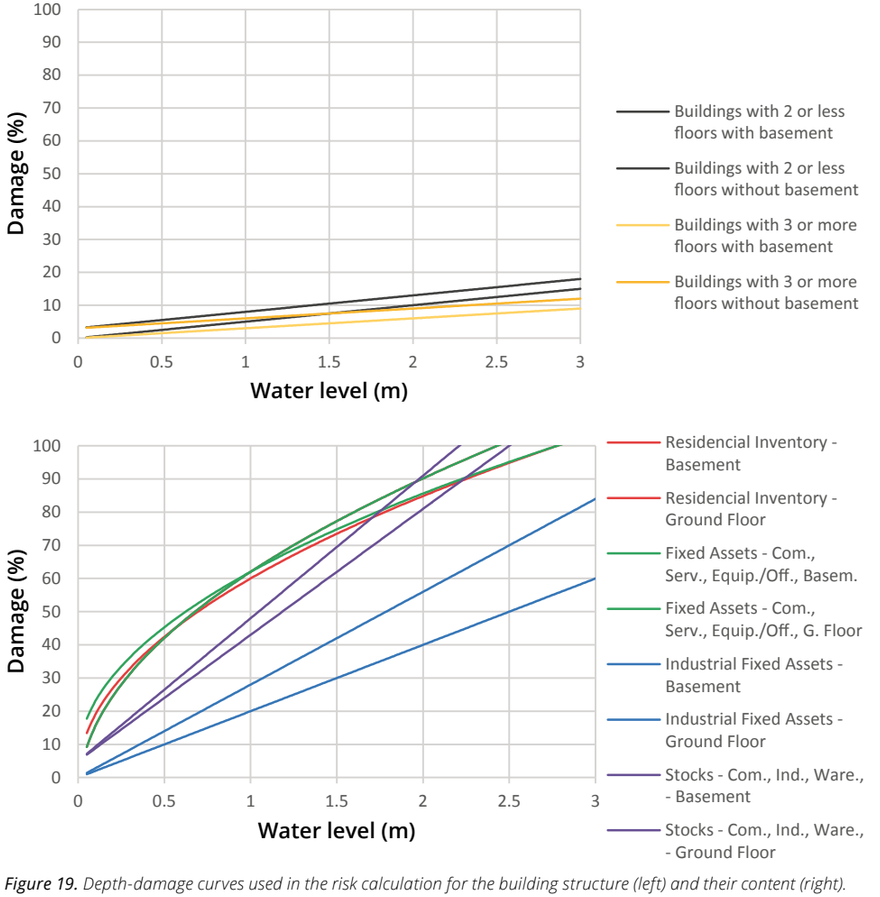

Figure 19. Depth-damage curves used in the risk calculation for the building structure (left) and their content (right). Source: adapted from Markau (2003) and Reese et al. (2003).

Table 15. Mathematical expressions used in each damage category in the risk assessment, where Y corresponds to the damage percentage and x to the water level (in centimeters). Source: adapted from Markau (2003) and Reese et al. (2003).

Damage Category				Function
Structure[xxiv]		Building with two floors or less	No basement	$Y = 5x$
			Basement	$Y = 3 + 5x$
		Building with three floors or more	No basement	$Y = 3x$
			Basement	$Y = 3 + 3x$
Content		Residencial Inventory[xxv]	Basement	$Y = 68\sqrt{x} - 6$
			Ground floor	$Y = 60\sqrt{x}$
	Fixed Assets[xxvi]	Comerce, services, offices and equipments	Basement	$Y = 68\sqrt{x} - 6$
			Ground floor	$Y = 57\sqrt{x} + 5$
		Industrial buildings	Basement	$Y = 28x$
			Ground floor	$Y = 20x$
		Stocks – comerce, industrial, warehouses	Basement	$Y = 5 + 43x$
			Ground floor	$Y = 3 + 38x$

for defining damage curves in Portugal. Therefore, the curves adopted in this guide are the result of the literature and expert judgment in this area, and this survay was performed in order to choose those which have a better suit to the national reality. Thus the curves applied are adapted from the study "*Micro-scale study of the Risk Evaluation of Flood-prone Coastal Lawlands*" (see e.g. Meyer and Messner, 2005 Sterr et al., 2005). By applying these curves, percentages of damage associated with the level of the flood water, are obtained. For this reason, these curves are referred to as depth-damage curves.

Each curve shown in Figure 19 has a mathematical formula to be applied depending on the characteristics of elements to be evaluated. These are shown in Table 15 where the damage categories are divided into structure and contents of the building. The formulas associated with the structure, calculate the damage for the entire building, while the formulas associated with content enable the differentiation of calculating the damage to the ground floor or to the basement floor depending on where a particular activity is performed.

With the definition of damage curves and having previously conducted a survey of the exposed elements and the hydrological modeling with results for water level at different return periods, the information necessary for the operation of the risk assessment is gathered. This assessment is typically performed using geographic information systems (GIS). The methodology described below is based on the case study of downtown Lisbon for the damage category of commerce fixed assets, services, offices

xxiv *The term building structure should be interpreted broadly, comprising in addition to the structural elements of the buildings, their walls, coatings, supply networks and other elements that are an integral part of the building.*

xxv *Residential inventory is defined as all goods that are inside of a fraction with residential use.*

xxvi *Real estate located permanently within a fraction or building, (eg. Industrial machines, servers, cold rooms, etc.)*

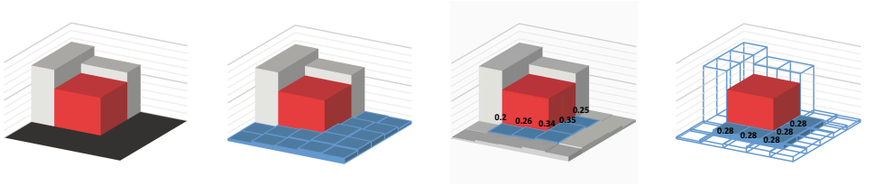

Figure 20. Example of the effect of the level of the water to the building. The red represents a determined-building and the blue the pixels that contain the water level (in centimeters). (a) buildings without flooding (b) buildings with grid where the level of water is stored, (c) selecting the pixel of the grid close to the building, (d) average calculation of the selected pixels in (c). Source: production of the author.

and equipment located on the ground floor - hereinafter referred to as non-industrial fixed assets (Ground Floor).

The first step of risk assessment is the assignment of water level, obtained through hydrological modeling, exposed to the elements, which in this particular case are the buildings.

Bearing in mind that in a GIS the level of the water in a flood, obtained by any hydrodynamic model, is stored in a grid structure and buildings are represented by polygons, it is necessary to execute some procedures for the allocation of values of that grid to polygons. Taking as example a single building overlaid on the water level information, there will be several pixels on the grid which are contiguous or near the polygon representing this building (Figure 20 - b). The nearest values to this polygon will be those that will affect it in this flood scenario. In this sense these pixels are selected (Figure 20 - c) to calculate the average value of the water level in the building (Figure 20 - d). This value is then assigned to the polygon representing the building. Note that the location and number of selected pixels for a given building must be equivalent for all return periods evaluated.

After this operation and the direct application of the function that describes the depth-damage curve to different polygons that contain the average level of the flood water, a percentage of damage is obtained. Taking as an example the curve for the damage category of non-industrial fixed assets (Ground Floor) - described in Table 16, the damage from the flood depicted in Figure 20 equals $68\sqrt{0.28} - 6$. This equates to an approximate damage equal to 30% of the total of non industrial fixed assets present on the ground floor of this building. This calculation must be performed for all buildings of the basin where the referred economic activities are present.

Table 16. Damage function for calculating the risk of non-industrial assets (Ground Floor).

Damage Category				Function
Content	Ativos fixos	Comércio, serviços, escritórios, etc.	R/C	$Y = 68 + \sqrt{x} - 6$

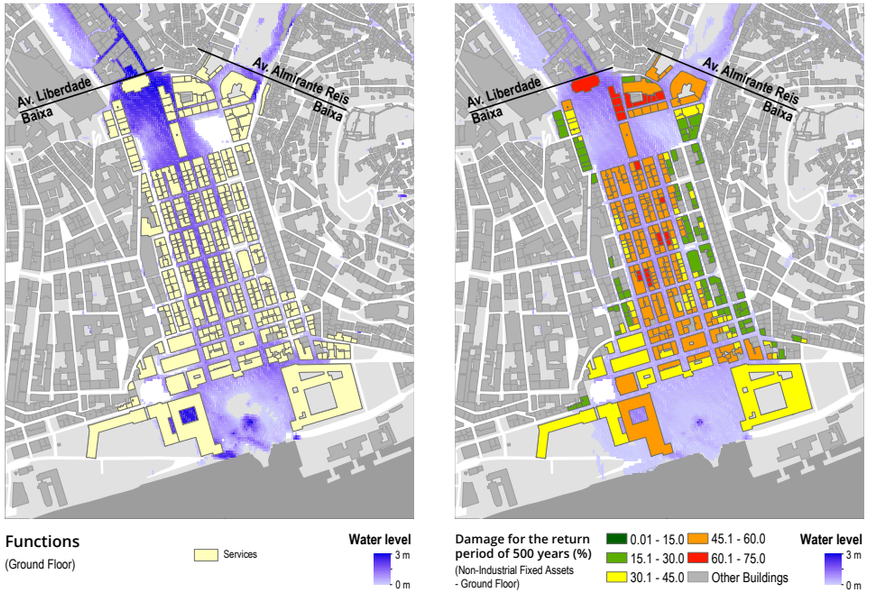

Figure 21. Selection of buildings with activities of commerce, services, equipment and offices located on the ground floor (a). Application of damage curve on fixed assets - commerce, services, equipment and offices located on the ground floor to the water level of a flood with a return period of 500 years (b). Source: production of the author using data from the Lisbon City Hall and hydrodynamic modeling.

To illustrate the necessary procedures for the damages calculation in a small dimension basin using a GIS, it was taken as example the Lisbon downtown, for a flood with a return period of 500 years and a damage category of non industrial fixed assets (Ground Floor). The procedures needed for that calculation are illustrated in Figure 21, being carried out after the allocation of the water level to the buildings for the return period of 500 years. In this figure image (a) corresponds to the selection of buildings where there are no industrial fixed assets on the ground floor and image (b) results of applying the function of Table 16 to the previously selected buildings.

This operation allows to obtain the expected damage to a flood with a return period of 500 years, which for the illustrated case varies between 0 and 75% in buildings with no industrial activities associated with the ground-floor. The average damage in downtown Lisbon for an event of this magnitude and this category of damage is 44.66 %. Theoretically, to calculate the risk of flooding associated with this return period, it would be necessary to multiply the damage obtained for each building by the probability of occurrence of the event. This operation will distribute the damage value by the number of years that, on average, the flood takes to occur. However, what would be obtained would

only consist of the average annual damage of a flood with these criteria and not the average of all flood damage that may occur in this section of the basin. This objective is achieved by building - probability damage curves, a process that will be explained in more detail in the next section.

calculation of the average annual damage

The calculation of the average annual damage resulting from flooding is obtained through an approach that seeks to represent all events that theoretically might occur in a given basin. This approach results in the construction of probability-damage curves (Meyer et al., 2009a). As mentioned the average damage for a return period of 500 years of non-industrial assets (Ground Floor) for the section of the basin illustrated is 44.66%. If you put this value in a graphic where the ordinates axis corresponds to the percentage of damage, and the abscissa to the different probabilities associated to the return periods assessed (which in this case are the probabilities of non exceedance of 0.5, 0.2, 0.1, 0.05, 0.02, 0.01 and 0.002) it results in the first point of the probability-damage curve (Figure 22).

The remaining points will be obtained by calculating the average damage of the area to the associated moduled floods with different return periods. The method for these calculations is identical to that described for the return period of 500 years, and its results for the return period of 10, 50 and 100 years are presented in Figure 23. The average damage values for these return periods in the damage category of non-industrial fixed assets (Ground floor) are respectively of 6.74%, 26.94% and 18.46%. The remaining values associated with return periods assessed correspond to 2.02% (2 years), 4.3% (5 years) and 15.85% (20 years).

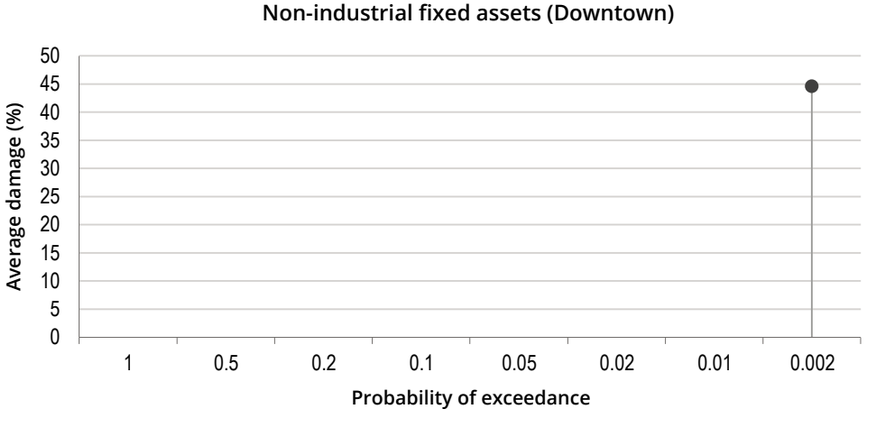

Figure 22. Graphical representation of the average damage of non-industrial assets (Ground Floor) for a return period of 500 years. Source: production of the author.

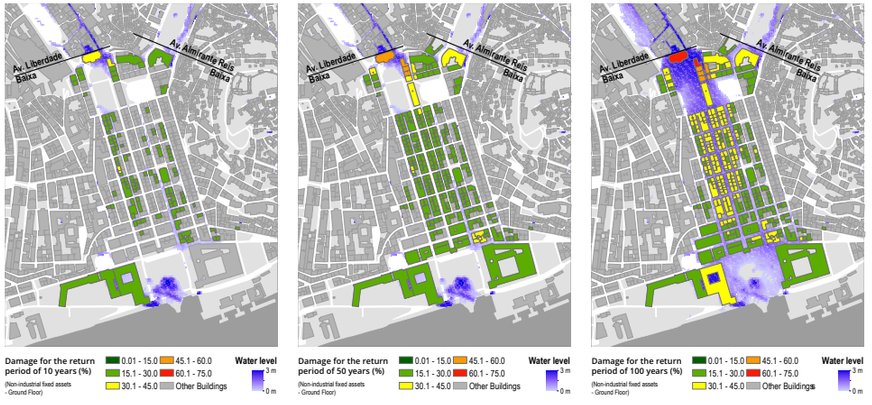

Figure 23. Damage calculations for different return periods (10, 50 and 100 years). Source: production of the author using data from the Lisbon City Hall and hydrodynamic modeling.

After the quantification of damages for all return periods moduled and the respective averages of the damage in the area under assessment, there is all the data needed to complete the construction of the probability-damage curve of Figure 23. Placing on this map the remaining damage values in accordance with the probability of non exceedance referred, results in seven points which, after interpolation, provides the damage curve for non-industrial fixed assets located on the ground floor of the buildings of downtown Lisbon (Figure 24).

Usually the flood with a return period of two years is modeled to confirm that the values of that precipitation do not have any consequence on the risk assessment. Having verified this situation the probability-damage curve has its beginning in the probability of exceedance associated with this return period. In the case of the section of the basin under study it appears that on this return period there is already damage, meaning that the curve has its beginning in a period of higher frequency. This situation is related to some rainwater collectors of Lisbon already identified in previous studies (see EMARLIS, 2007) coming into load.

When the probability-damage curve does not have a null value for the payback period of 2 years it may be chosen different approaches to overcome this situation. One possibility is the assumption that even after checking the existence of damage in this return period , the curve ends on this point (see eg Veerbeek and Zevenbergen 2009, Ernst et al., 2010), accepting the underestimation of the average annual damages value that it arises (approach (b) of Figure 25). Another possibility is the extension of the curve to the theoretical return period of one year attributing the average damage value of zero to this point, assuming an overestimation of the damage (approach (a) of Figure 25). Although these approaches allow an approximation to the average annual damages, it is convenient to obtain the probability from which the damage is effectively zero, implying nonetheless an increased number

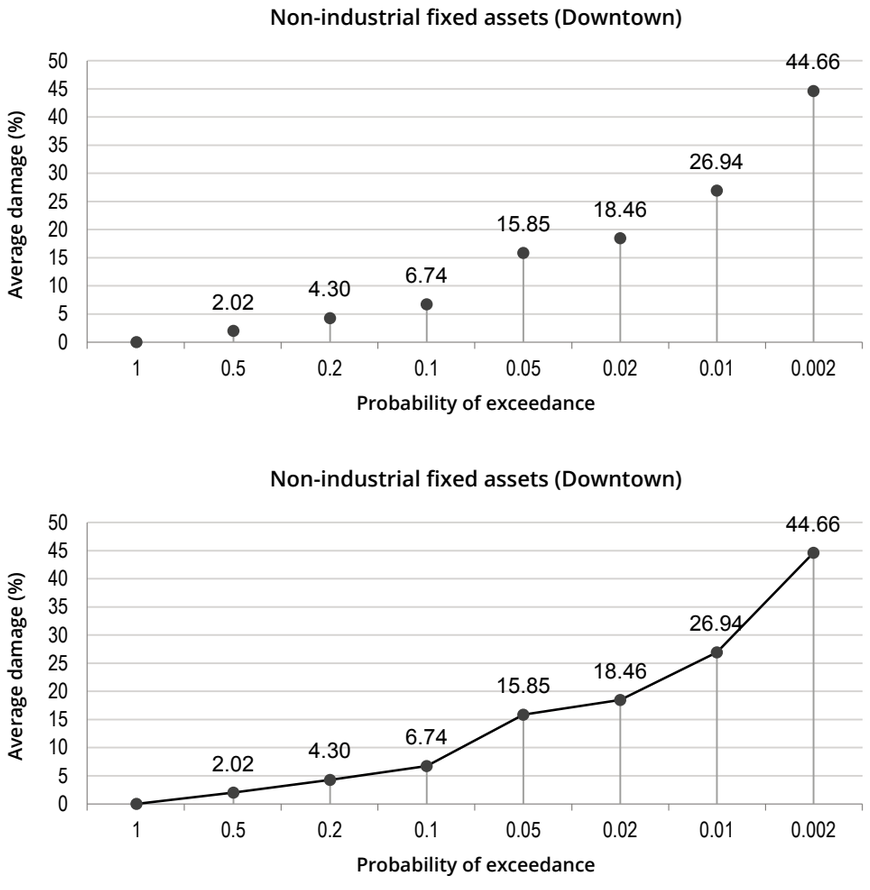

Figure 24. Damage values associated with different probabilities of occurrence (left) and its interpolation to define the probability curve of non-industrial fixed assets – Ground floor (right). Both graphics have a linear scale assigned to the abscissa axis. Source: production of the author).

of return periods to be taken into account in the risk assessment (Ward et al., 2011).

After constructing the probability damage curve it can be calculated the annual average damage of the damage category that this curve refers to. As mentioned in section 2.5.6 this average annual damage is obtained by calculating the area that is below the damage probability curve. There are different approaches to this calculation. The first of which consists of calculating the integral of the function which defines the curve. In this case it is necessary to define this function using a graphic where both axes have a linear scale, and where

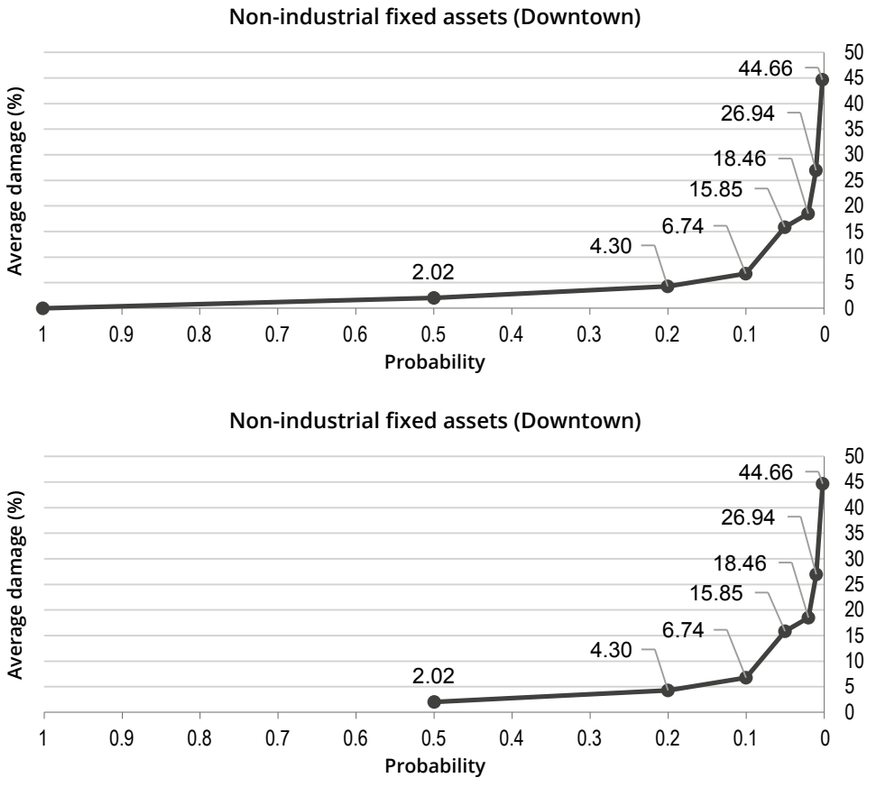

Figure 25. Probability damage curves for non-industrial assets (ground floor) located in downtown Lisbon following the approach (a) - left - and (b) - right. Both graphics have a linear scale assigned to the abscissa axis. Source: production of the author.

the curve is represented. Exemplifying this approach are the graphics shown in Figure 25. However and as also noted above, it is more usual to resort to an approximation of the calculation of this area by using equations (7) and (8).

Table 17 summarizes the procedures to be adopted for obtaining the average annual damage, taking as an example the category of non-industrial fixed assets damage (Ground floor). In this case, it is expected an annual loss of around 3.6% of total industrial fixed assets not located on the ground floor of buildings present in the part of the basin corresponding to downtown Lisbon. However, these figure results of the individual assessment of each building, which was held in a GIS environment, making it possible to spatialize the information and present the risk assessed for each building (Figure 26).

Table 17. Example of calculation required to obtain the annual average damage from non-industrial assets (ground floor), applied to the approach (a). [xxvii] The figures are rounded to the second decimal place.

i	Probability (P)	Damage (D)	$D[i]=\frac{D(P_{i-1})+D(P_i)}{2}$	$\Delta P[i]=\lvert P_i-P_{i-1}\rvert$	$D[i]\times\Delta P_i$
1	0.5	2.02	1.01	0.5	0.51
2	0.2	4.30	3.16	0.3	0.95
3	0.1	6.74	5.52	0.1	0.55
4	0.05	15.85	11.28	0.05	0.56
5	0.02	18.46	17.16	0.03	0.51
6	0.01	26.94	22.7	0.01	0.23
7	0.002	44.66	35.8	0.008	0.29
				$\bar{D}=\sum_{i=1}^{K} D[i]\times\Delta P_i=$	3.60

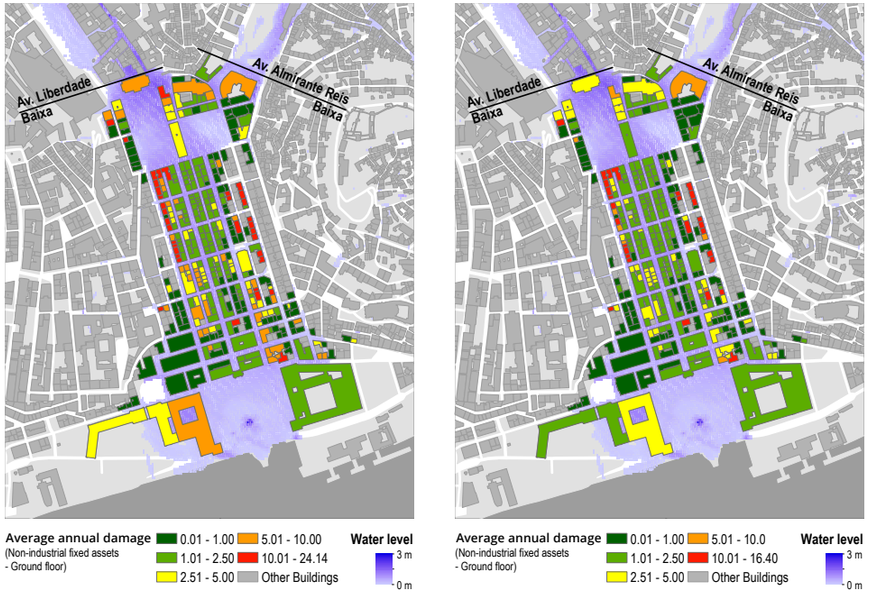

Figure 26. Average annual damage obtained by proximity (a)-left - and (b) - right - for every downtown building potentially affected by floods. Source: production of the author using data from the Lisbon City Hall and hydrodynamic modeling.

xxvii *In order to obtain the value of* $D[1]$ *and* $P[1]$ *it was considered that* $D_0=0$ *and* $P_0=1$ *as described for the approach (a).*

Concluded the quantification of loss on this damage category it will be necessary to apply all the steps described for this quantification to other categories that are ment to be evaluated. In the case that serves as an exemple for this guide (Table 15) it will still have to be calculated the damage to the fixed assets located in the basement of the buildings as well as industrial fixed assets, the residential inventory and stocks. These three damage categories have to be evaluated separately for the basement and the ground floor just as it happens to industrial fixed assets. It remains to be mentioned the damage category associated with the building structure shown in Table 15. There are four formulas to be applied on this one, depending on the number of floors and the absence or presence of basements. The quantification of damage in this category results from direct application of the formula corresponding to the characteristic of the building in question (taking into account the number of floors and the presence or absence of basements), as the remaining procedures are identical to the other damage categories.

results to be obtained

Table 18 summarizes the results of applying this methodology to all categories of damages. This table presents the values corresponding to the downtown area which illustrate this guide and also the results corresponding to those portions of the basin that develop along the Avenida da Liberdade and Avenida Almirante Reis. Note that the damage is not exclusive of these two avenues, incorporating all the areas that surround them and which together correspond to the sub-basin of Avenida da Liberdade and Avenida Almirante Reis. There were still included the totals of the entire basin.

For each damage category it is possible to spatialize information through risk maps as exemplified for non-industrial assets (ground floor) in Figure 26. Though it may be considered that the risk assessment is completed, some authors still propose ways to add any information about different components of damage in a single map or display (see eg Meyer et al., 2009c).

aggregation of damage categories.

Implementation of such aggregation is achieved by assigning weights to each of these damage categories that reflect its importance relatively to the other. Usually it results from surveys with experts, and there are several ways to do this. The most suitable is to carry out individual inquiries, although the group interviews are also possible but with major limitations due to biases caused by the influence of certain people over others (EC, 2004). The importance of this query is defined by many authors as the crucial point of the interested participants in risk analysis, in case you intend to aggregate information of damage on a single map or indicator (see eg Bruijn et al., 2009 Schmidt-Thomé et al., 2006).

There are several methods to define the weights for each criterion (see Malczewski, 1999). Below are illustrated the procedures for the application of only one of these methodologies. This methodology is called *pairwise comparison method* (PCM) for multiple decision makers and was chosen as one of the most appropriate in this context (Malczewski, 1999).

Table 18. *Result of the calculation of the average annual damage for the different damage categories applied to the part of the basin under assessment. It shows the values for the entire basin and disaggregated by sub-basins (Downtown area, Av. Liberdade and Av. Almirante Reis). In the column referring to damage, the first value presented to a particular category, was obtained by approach b)[xxviii] and the second through approach (a). The average annual damage values are rounded to the second decimal place.*

	Total of the basin		Downtown		Av. Liberdade		Av. Almirante Reis	
	Damage (%)	Exposed elements	Damage (%)	Exposed elements	Damage (%)	Exposed elements	Damage (%)	Exposed elements
Structure of building	0.13 0.18	1001	0.04 0.06	368	0.22 0.29	285	0.14 0.20	348
Residencial Inventory Basement	0.02 0.04	1	0	0	0.02 0.04	1	0	0
Residencial Inventory Ground Floor	4.38 6.28	103	4.03 5.92	2	4.13 5.94	37	4.53 6.50	64
Non-industrial fixed assets Basement	4.22 6.00	16	2.78 3.69	2	4.20 5.97	9	4.82 6.98	5
Non-industrial fixed assets Ground Floor	4.62 6.75	853	2.42 3.60	363	7.37 10.57	230	5.27 7.75	260
Industrial fixed assets Basement	0.03 0.05	1	0	0	0	0	0.03 0.05	1
Industrial fixed assets Ground Floor	0	0	0	0	0	0	0	0
Stocks Ground Floor	2.44 3.47	53	0.72 1.1	4	2.72 3.83	27	2.40 3.45	22
Stocks Basement	2.07 2.94	782	1.02 1.48	318	3.32 4.59	220	2.31 3.34	244

The PCM is a two-way table where each participant is asked, to choose what the importance of one element is over another. Table 19 illustrates the manner of filling the table for damage category, in this case, the structure of the building. Being a procedure for multiple decision makers are, it is asked to each expert to fill in table

xxviii *This approach is not explored in detail in this document, being however noted that the results obtained do not result directly from the curve shown in Figure 25, which only aims to illustrate this approach. This approach only accounts for damages from the return period on which a building is affected. As an example if a building is impacted from the return period of 50 years, then the curve of that building only begins at that point. The values in Figure 25 illustrate the approach (b) and do not reflect such situations. However, the values accounted for, in all the results of this approach throughout this document reflect those situations.*

cells with a value of 1 (most important) and 0 (least important) by their opinion, being their analysis made of the damage category identified in each column relative to the line. As an example and observing Table 19, if the interviewee considers that the building structure is more important than the residential inventory then he should assign the value 1 to the cell that lies at the intersection of column of the structure of the building (a) with the line of the residential inventory (2) and the value 0 to the cell at the intersection of the column residential inventory (b) with the line of the structure of the building (1).

The interviewee must pay particular attention to the fact that it is relatively easy to give incoherent answers when filling the matrix. As an example, the interviewee may state that, by completing the matrix, the structure of the building is more important than the residential inventory and that the residential inventory is more important than

Table 19. Matrix investigation to be completed for the application of the pairwise comparison method. Source: adapted Malczewski (1999)

	Structure of building (a)	Residencial Inventory (b)	Non-industrial fixed assets (c)	Industrial fixed assets (d)	Stocks (e)
Structure of building (1)	0	0	1	1	0
Residential inventory (2)	1	0	—	—	—
Non-industrial fixed assets (3)	0	—	0	—	—
Industrial fixed assets (4)	0	—	—	0	—
Stocks (5)	1	—	—	—	0
Position	∑a=2	∑b	∑c	∑d	∑e

Table 20. Matrix filled in with the result of 12 surveys of experts in the area of flood insurance.

	Structure of building (a)	Residencial Inventory (b)	Non-industrial fixed assets (c)	Industrial fixed assets (d)	Stocks (e)
Structure of building (1)	0	4	8	10	10
Residencial Inventory (2)	8	0	12	12	12
Non-industrial fixed assets (3)	4	0	0	8	5
Industrial fixed assets (4)	2	0	4	0	1
Stocks (5)	2	0	7	11	0
Position	16	4	31	41	28

the non-industrial fixed assets. However, the same interviewee in the same matrix may indicate that these fixed assets are more important than the building structure. This order of importance given to the damage categories is theoretically impossible, making the matrix inconsistent. This involves paying careful attention to the filling in; otherwise the survey can not be considered to perform the aggregation of damages.

After obtaining a determined number of consistently completed inquiries, all obtained responses are added in each cell of the grid. The result of this operation is shown in Table 20 with real data obtained from a survey of 12 experts who perform their professional activity in the insurance business.

The next step in the process of obtaining the weight to be given to the damage categories consist of the sum of each column of the matrix for each criteria. This operation results in a classification of the importance of damage categories, although not yet standardized (Table 20)

To proceed with the standardization of these weights it is necessary to perform some operations that are intended to be illustrated in Table 21.

Table 22 shows the values obtained for the survey carried out through the operation of the procedures described in Table 21.

Obtained the weights for each criteria, it is calculated the aggregate risk for the area under study. Since in this particular case, the average annual damage is calculated separately for the ground floor and the basement, and the weights obtained do not

Table 21. Matrix of procedures for the calculation of the weights assigned to each damage category, with the goal of building a single map or indicator that reflects the overall risk of an area. The value ***n*** *corresponds to the number of surveys. Source: adapted from Malczewski (1999).*

Damage category	Classification	Class	Wight
Structure of building	∑a	a'=∑a/(nc-n)	a'/Domínio
Residencial Inventory	∑b	b'=∑b/(nc-n)	b'/Domínio
Non-industrial fixed assets	∑c	c'=∑c/(nc-n)	c'/Domínio
Industrial fixed assets	∑d	d'=∑d/(nc-n)	d'/Domínio
Stocks	∑e	e'=∑e/(nc-n)	e'/Domínio
	∑ = nc	∑ = Domínio	∑ = 1

Table 22. Calculation matrix of the weight of the damage categories based on 12 surveys. The figures are rounded to the third decimal place.

Damage category	Classification	Class	Weight
Structure of building	16	0.148	0.133
Residencial Inventory	4	0.037	0.033
Non-industrial fixed assets	31	0.287	0.259
Industrial fixed assets	41	0.380	0.342
Stocks	28	0.259	0.233
	120	1.111	1

make this discrimination, it is necessary to calculate the average value of each damage category related to the content. That is, taking as an example the non-industrial fixed assets and assuming that a building has the underlying activities to that category on the ground floor and in the basement, the two values found for that building shall be added together and the result divided by two. Meanwhile, if a building only has a value that matches this category, corresponding to the basement or ground floor, then this value is assigned without any operation. This calculation must be performed for all damage categories with the exception of the building structure, which already accounts for an average value for the entire building.

If the same calculations are performed for the entire basin and for the sections of Avenida da Liberdade and Avenida Almirante Reis each of the areas can be compared and conclude which presents the highest risk, taking into account the different damage categories evaluated (Table 24).

This information can be spatialized, originating aggregated risk maps. Figure 27 presents two examples of these maps for downtown Lisbon, consisting of the final results of the risk assessment process.

It is noteworthy that the process of aggregation of different damages allows an immediate reading of the risk associated with the area under study, after being known the assumptions of its assessment, that for the given example consist of the examination of the different damage categories. On the other hand, the risk assessment may end with the collection and mapping of damage to their different categories. This information consists of the average annual damage of a certain category associated with a building or area, which can vary between 0 (no loss) and 100 % (total loss). If it is known the total value of that

Table 23. Calculating the aggregated risk of the average annual damage obtained for the area of downtown Lisbon using the approach (a). The value of average annual damage of the structure of the building is equal to the value shown in Table 17 for this approach. The remaining values were calculated using a GIS as described above. The values presented are rounded to three decimal places.

Damage category	Damage, approach (a)	Weigth	Weighted damage
Structure of building	0.058	0.133	0.008
Residencial Inventory	0.032	0.033	0.001
Non-industrial fixed assets	3.548	0.259	0.919
Industrial fixed assets	0	0.342	0
Stocks	1.284	0.233	0.299
		Aggregate risk =	1.227

Table 24. Result of aggregate risk for the all the basin under study and three areas contained in this basin. It is concluded through this table that the area most at risk is Avenida da Liberdade. The figures are rounded to the second decimal place.

Aggregate risk	Total basin	Downtown	Av. Liberdade	Av. Almirante Reis
Approach (a)	2.07	1.23	3.11	2.11
Approach (b)	1.43	0.83	2.19	1.45

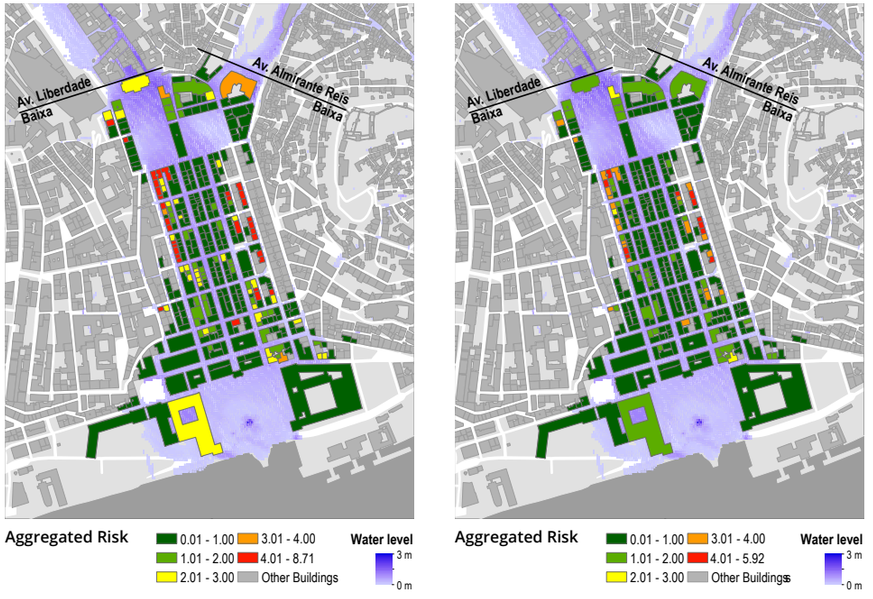

Figure 27. Aggregation of average annual damage to the calculation modules b (left) and a (right). Source: production of the author using data from the Lisbon City Hall and hydrodynamic modeling.

category for the rated universe, then that percentage can be converted into monetary values. With all percentages of average damage converted into monetary values, it is no longer relevant the aggregation process presented in this guide as the overall risk (represented in this guide as the aggregate risk) it is not more than the sum of all the values found for the building or for the evaluated areas.

FINAL REMARKS

"It doesn't matter if the water is cold or warm
if you're going to have to wade through it anyway."

Pierre Teilhard de Chardin

This paper presents a methodology for quantifying the risk of flooding, addressing the processes that allow to define the probabilities and consequences inherent to risk assessment. These methods have become increasingly more important, combining information that can be gathered into three major groups that present, in this context, a high level of interconnections between them. These groups consist of i) the meteorological and hydrometric data, ii) the hydrological modeling and iii) susceptibility of the exposed elements.

Procedures are presented under the first group to define the return periods of annual maximum daily precipitation and, on this basis, the construction of hyetographs. The return periods are obtained by using the extreme values theory, comparing the result of applying the Gumbel Distribution and Pearson Law III to the values of annual maximum daily precipitation of IGIDL meteorological station, located in Lisbon. It was calculated, for both laws, the confidence intervals of the estimated values in order to evaluate the uncertainty associated with this estimation. However it was not considered in this estimation other statistical laws that can be used, as the Log- Pearson III distribution or the Generalized Extreme Value distribution. In this first group, there are also included hydrometric data, if available, that can be used for the estimation of maximum instantaneous flow and flooded areas, as well as for purposes of calibration and validation of hydrodynamic models.

The hydrological basin that underpins this document does not have available measurements of flows disabling its statistical treatment. Moreover hydrodynamic modeling is not detailed in this guide, given the complexity of processes inherent to this procedure, which prevents a detailed analysis, for example, of procedures for calibration and validation of these models, which may be important for the quality of obtained results.

The second group relates to the hydrodynamic modeling. This document is explicit in terms of what are the needed steps to operationalize these models and their influence on the results. The hydrodynamic models require several input data including information of land use and occupation, digital terrain models, soil types, drainage networks etc. These data are not always available with the detail and completeness required. On the other hand, the more detailed and comprehensive information is, the greater will be the processing time of the hydrodynamic models. This implies a commitment that has consequences on the level of confidence associated with the estimation of the different characteristics of the flood resulting from the modeling (eg., flooded area and water level). Note that this situation is not unique to this group since, and as mentioned, the return periods themselves have a degree of uncertainty associated to its estimation.

The third group is referred to generically as the susceptibility of the exposed elements. This document and for this group of indicators are defined and exemplified methodologies related to the gathering of the elements exposed and characterization of susceptibility of these elements. This susceptibility is usually quantified through damage curves consisting of graphic representations of expected damage for a given object or set of objects, as a result of a specific characteristic of flood. After defining the damage categories to be assessed, depth-damage curves were chosen and applied systematically to a specific section of the basin that illustrates this document and the necessary calculations to obtain the average annual damage of these categories. Nevertheless, it is presented results of the 5 damage categories assessed for the entire hydrographic basin and three sub-basins that constitute it (Downtown, Avenida da Liberdade, Avenida Almirante Reis). After these operations, it is still suggested a way to aggregate all the information generated in a single map or display, aiming at an immediate reading of the risk associated with the whole basin or part of it. However it should be noted that this aggregation does not replace the different results obtained for the average annual damage in the different categories studied, so it should be seen as complementary information to these results.

Although the majority of studies conducted in Europe to evaluate flood risk use damage curves, the formulation of these curves is coated with a certain level of uncertainty. These curves are obtained through historical records of damage on the exposed elements, and there is not this type of systematic registration for Portugal. Therefore it was necessary to resort to information from other studies increasing the uncertainty associated with this process. It remains to mention that the calculation necessary for obtaining the risk of flooding is fairly stabilized.

In summary this guide is a systematic approach to the calculation of flood risk procedure and presents a possible approach for this purpose. This approach conforms to the state of the art in this subject, and there are some uncertainties to take into account in the results obtained.

acknowledgements

The authors would like to thank i) Professora Maria Manuela Portela, Professor Saldanha Matos, Professora Maria Clara Mendes, Professor Filipe Duarte Santos, Professor Ramiro Neves and Engenheiro David Brito for sharing their knowledge about the most diverse subjects contained herein; ii) Lisbon City Council, Oeiras City Council and Municipia SA for supplying geographic information at municipal level; iii) monitoring commission of the CIRAC project ; iv) Foundation for Science and Technology for the award of the PhD grant with reference SFRH/BD/70435/2010, under which this document is performed.

BIBLIOGRAPHY

"I love the sounds and the power of pounding water, whether it is the waves or a waterfall."

Mike May

1. ANDRADE, C., PIRES, H. O., SILVA, P., TABORDA, R. & FREITAS, M. D. C. 2006. Zonas Costeiras. In: SANTOS, F. D. & MIRANDA, P. (eds.) Alterações Climáticas em Portugal Cenários, Impactos e Medidas de Adaptação, Projecto SIAM II. Lisboa: Gradiva.
2. BLADÉ, I., CACHO, I., CASTRO-DÍEZ, Y., GOMIS, D., GONZÁLEZ-SAMPÉRIZ, P., MIGUEZ-MACHO, G., FIZ, P., RODRÍGUEZ-FONSECA, B., RODRÍGUEZ-PUEBLA, C., SÁNCHEZ, E., MARCOS, G. S., VALERO-GARCÉS, B. & VARGAS-YÁÑEZ, M. 2010. Clima en España: Pasado, presente y futuro - Informe de evaluación del cambio climático regional. Fiz F. Pérez y Roberta Boscolo; Mº de Medio Ambiente y Medio Rural y Marino, Mº de Ciencia e Innovación.
3. BRANDÃO, C., RODRIGUES, R. & COSTA, J. P. D. 2001. Análise de Fenómenos Extremos - Precipitações Intensas em Portugal Continental. Lisboa: Direcção dos Serviços de Recursos Hídricos.
4. BRUIJN, K. D., KLIJN, F., ÖLFERT, A., PENNING-ROWSELL, E., SIMM, J. & WALLIS, M. 2009. Flood risk assessment and flood risk management. An introduction and guidance based on experiences and findings of FLOODsite (an EU-funded Integrated Project), Delft, the Netherlands, Deltares | Delft Hydraulics.
5. CE 2004. A Análise da Informação: Inquéritos Delphi. EVALSED - A Avaliação do Desenvolvimento Socioeconómico - Manual Técnico II: Métodos e Técnicas de Avaliação Lisboa: Observatório do QREN, Comissão Europeia.
6. CHOW, V. T. 1954. The log-probability law and its engineering applications. Proceedings of the American Society of Civil Engineers, 80, 1-25.
7. DE MOEL, H. & AERTS, J. 2010. Effect of uncertainty in land use, damage models and inundation depth on flood damage estimates. Natural Hazards, 1-19.
8. DE MOEL, H., VAN ALPHEN, J. & AERTS, J. C. J. H. 2009. Flood maps in Europe - methods, availability and use. Nat. Hazards Earth Syst. Sci., 9, 289-301.
9. DECRETO LEI N.º 115/2010 2010. Estabelece um quadro para a avaliação e gestão dos riscos de inundações, com o objectivo de reduzir as suas consequências prejudiciais, e transpõe a Directiva n.º 2007/60/CE, do Parlamento Europeu e do Conselho, de 23 de Outubro. Diário da República,1.ª série - Nº 206, Decreto-Lei n.º 115/2010.
10. DIAS, L. 2013. City, climate change and floods. A contribution to the urban resilience study. In: KLIJN, F. & SCHWECKENDIEK, T. (eds.) Floodrisk 2012 – The 2nd European Conference on Flood Risk Management - Comprehensive Flood Risk Management. Rotterdam: CRC Press, Taylor & Francis Group.
11. DIRECTIVA 2007/60/CE 2007. Directiva do Parlamento Europeu e do Conselho, de 23 de Outubro de 2007, relativa à avaliação e gestão dos riscos de inundações.
12. DUTTA, D., HERATH, S. & MUSIAKE, K. 2003. A mathematical model for flood loss estimation. Journal of Hydrology, 277, 24-49.
13. EEA, WHO & JRC 2008. Impacts of Europe's changing climate—2008 indicator-based assessment, Copenhagen, Denmark, European Environment Agency.
14. EMARLIS 2007. Plano Geral de Drenagem de Lisboa - Fase C: Desenvolvimento do Plano Geral de Drenagem. Miraflores: ChiRoN, Engidro, Hidra.

15. ERNST, J., DEWALS, B., DETREMBLEUR, S., ARCHAMBEAU, P., ERPICUM, S. & PIROTTON, M. 2010. Micro-scale flood risk analysis based on detailed 2D hydraulic modelling and high resolution geographic data. Natural Hazards, 55, 181-209.
16. EXCIMAP 2007. Handbook on good practices for flood mapping in Europe. EU: European exchange circle on flood mapping.
17. FEKETE, A. 2010. Assessment of Social Vulnerability to River Floods in Germany, Bonn, University Institute for Environment and Human Security (UNU-EHS).
18. GOULDBY, B. & SAMUELS, P. 2005. Language of risk—project definitions. Integrated Flood Risk Analysis and Management Methodologies. Floodsite Project Report T32-04-01.
19. IPCC 2012. Managing the Risks of Extreme Events and Disasters to Advance Climate Change Adaptation - Special Report of the Intergovernmental Panel on Climate Change. In: FIELD, C. B., BARROS, V., STOCKER, T. F., DAHE, Q., DOKKEN, D. J., EBI, K. L., MASTRANDREA, M. D., MACH, K. J., PLATTNER, G.-K., ALLEN, S. K., TIGNOR, M. & MIDGLEY, P. M. (eds.) Cambridge Univeristy Press ed.: First Joint Session of Working Groups I and II.
20. IPCC 2013. Climate Change 2013: The Physical Science Basis (Final Draft Underlying Scientific-Technical Assessment). Intergovernmental Panel on Climate Change.
21. ISO 31010 2009. ISO/IEC 31010:2009 - Risk management - Risk assessment techniques. ISO/IEC.
22. JONKMAN, S. N., KOK, M. & VRIJLING, J. K. 2008. Flood Risk Assessment in the Netherlands: A Case Study for Dike Ring South Holland. Risk Analysis, 28, 1357-1374.
23. JULIÃO, R. P., NERRY, F., RIBEIRO, J., BRANCO, M. C. & ZÊZERE, J. 2009. Guia Metodológico para a Produção de Cartografia Municipal de Risco e para a Criação de Sistemas de Informação Geográfica (SIG) de Base Municipal, Lisboa, Autoridade Nacional de Protecção Civil.
24. KHARIN, V. V., ZWIERS, F. W., ZHANG, X. & HEGERL, G. C. 2007. Changes in Temperature and Precipitation Extremes in the IPCC Ensemble of Global Coupled Model Simulations. Journal of Climate, 20, 1419-1444.
25. KRON, W. 2005. Flood Risk = Hazard • Values • Vulnerability. Water International, 30, 58-68.
26. LEURIG, S. & DLUGOLECKI, A. 2013. Insurer Climate Risk Disclosure Survey: 2012 Findings & Recommendations. In: CERES (ed.). Boston: Ceres.
27. MALCZEWSKI, J. 1999. GIS and Multicriteria Decision Analysis, New York, Wiley.
28. MARKAU, H.-J. 2003. Risikobetrachtung von naturgefahren. Analyse, bewertung und management des risikos von naturgefahren am beispiel der sturmflutgefährdeten küstenniederungen schleswig-holsteins. Doktorgrades, Universität zu Kiel.
29. MARTINS, F. J. P. 2000. Dimensionamento hidrológico e hidráulico de passagens inferiores rodoviárias para águas pluviais. Mestre, Universidade de Coimbra.
30. MERZ, B., KREIBICH, H., THIEKEN, A. & SCHMIDTKE, R. 2004. Estimation uncertainty of direct monetary flood damage to buildings. Nat. Hazards Earth Syst. Sci., 4, 153-163.
31. MERZ, B., THIEKEN, A. H. & GOCHT, M. 2007. Flood Risk Mapping at the Local Scale: Concepts and Challenges. In: BEGUM, S., STIVE, M. J. F. & HALL,

J. W. (eds.) Flood Risk Management in Europe. Springer Netherlands.
32. MEYER, V., HAASE, D. & SCHEUER, S. 2009a. Flood risk assessment in european river basins—concept, methods, and challenges exemplified at the mulde river. Integrated Environmental Assessment and Management, 5, 17-26.
33. MEYER, V. & MESSNER, F. 2005. National flood damage evaluation methods — A review of applied methods in England, the Netherlands, the Czech Republic and Germany. Leipzig, Germany, Department of Economics, Umweltforschungszentrum Leipzig-Halle. UFZ-Discussion Papers.
34. MEYER, V., MESSNER, F., HAASE, D. & SCHEUER, S. 2009b. Developing methodological foundations for GIS-based multicriteria evaluation of flood damage and risk. FLOODsite project report T10-08-13.
35. MEYER, V., SCHEUER, S. & HAASE, D. 2009c. A multicriteria approach for flood risk mapping exemplified at the Mulde river, Germany. Natural Hazards, 48, 17-39.
36. MIN, S.-K., ZHANG, X., ZWIERS, F. W. & HEGERL, G. C. 2011. Human contribution to more-intense precipitation extremes. Nature, 470, 378-381.
37. MING-DAW SU, JUI-LIN KANG & LING-FANG CHANG 2009. Industrial and Commercial Depth-Damage Curve Assessment. Wseas Transactions on Environment and Development, 5, 199-208.
38. MRC/WUP-FIN 2008. Hybrid 1D/2D/3D model manual. Hydrological, Environmental and Socio-Economic modelling Tools for the Lower Mekong Basin Impact Assessment/ FINDS. Vientiane, Lao PDR: Mekong River Commission and Finnish Environment Institute Consultancy Consortium.
39. NAGHETTINI, M. & PINTO, É. 2007. Hidrologia Estatística, Belo Horizonte, CPRM.
40. NAGHETTINI, M. & PORTELA, M. M. 2011. Probabilidade e estatística aplicadas à hidrologia. Lisboa: DECivil, IST.
41. PALL, P., AINA, T., STONE, D. A., STOTT, P. A., NOZAWA, T., HILBERTS, A. G. J., LOHMANN, D. & ALLEN, M. R. 2011. Anthropogenic greenhouse gas contribution to flood risk in England and Wales in autumn 2000. Nature, 470, 382-385.
42. PORTELA, M. M., MARQUES, P. & CARVALHO, F. F. D. 2000. Hietogramas de projecto para a análise de cheias baseada no modelo do hidrograma unitário do Soil Conservation Service (SCS). In: HÍDRICOS, A. P. D. R. (ed.) 5° Congresso da água - A água e o desenvolvimento sustentável: Desafios para o novo século. Lisboa: Associação Portuguesa dos Recursos Hídricos.
43. REESE, S., MARKAU, H.-J. & STERR, H. 2003. Merk - Mikroskalige Evaluation der Risiken in überflutungsgefährdeten Küstenniederungen - Abschlussbericht. Ministerium für ländliche Räume, Landesplanung, Landwirtschaft und Tourismus des Landes Schleswig-Holstein.
44. SANTOS, F. D. & MIRANDA, P. 2006. Alterações Climáticas em Portugal Cenários, Impactos e Medidas de Adaptação - Projecto SIAM II, Lisboa, Gradiva.
45. SCHANZE, J. 2006. Flood risk management - A basic framework. In: SCHANZE, J., ZEMAN, E. & MARSALEK, J. (eds.) Flood Risk Management: Hazards, Vulnerability and Mitigation Measures. Springer Netherlands.
46. SCHANZE, J., ZEMAN, E. & MARSALEK, J. 2006. Flood Risk Management: Hazards, Vulnerability and Mitigation Measures Springer Netherlands.

47. SCHMIDT-THOMÉ, P., KALLIO, H., JARVA, J., TARVAINEN, T., GREIVING, S., FLEISCHHAUER, M., PELTONEN, L., KUMPULAINEN, S., OLFERT, A., BÄRRING, L., PERSSON, G., RELVÃO, A. M. & BATISTA, M. J. 2006. Spatial Effects and Management of Natural and Technological Hazards in Europe, ESPON 1.3.1.
48. SEC 2010. Risk Assessment and Mapping Guidelines for Disaster Management, 21.12.2010 - 1626 final. Brussels: Commission staff working paper.
49. STERR, H., MARKAU, H.-J. & REESE, S. 2005. Analyses of previous vulnerability studies in the pilot site German Bight Coast (Task 27). FLOODsite Status-Report.
50. TEMEZ, J. R. 1978. Calculo hidrometeorologico de caudales máximos en pequenas cuencas naturales. Madrid: Ministerio de Obras Publicas y Urbanismo, Direccion General de Carreteras.
51. THIEKEN, A. H., PETROW, T., KREIBICH, H. & MERZ, B. 2006. Insurability and Mitigation of Flood Losses in Private Households in Germany. Risk Analysis, 26, 383-395.
52. TRANCOSO, A. R., BRAUNSCHWEIG, F., CHAMBEL LEITÃO, P., OBERMANN, M. & NEVES, R. 2009. An advanced modelling tool for simulating complex river systems. Science of The Total Environment, 407, 3004-3016.
53. UNISDR 2004. Living with Risk. A global review of disaster reduction initiatives. United Nations International Strategy for Disaster Reduction Secretariat (UNISDR) ed. New York and Geneva: United Nations.
54. UNISDR 2009. UNISDR Terminology on Disaster Risk Reduction. In: NATIONS, U. (ed.). Geneva, Switzerland: United Nations International Strategy for Disaster Reduction (UNISDR).
55. VEERBEEK, W. & ZEVENBERGEN, C. 2009. Deconstructing urban flood damages: increasing the expressiveness of flood damage models combining a high level of detail with a broad attribute set. Journal of Flood Risk Management, 2, 45-57.
56. VICENTE-SERRANO, S., TRIGO, R., PEZ-MORENO, J., LIBERATO, M., LORENZO-LACRUZ, J., BEGUERERÍA, S., MORÁN-TEJEDA, E. & EL KENAWY, A. 2011. Extreme winter precipitation in the Iberian Peninsula in 2010: anomalies, driving mechanisms and future projections. Climate Research, 46, 51-65.
57. WARD, P. J., DE MOEL, H. & AERTS, J. C. J. H. 2011. How are flood risk estimates affected by the choice of return-periods? Nat. Hazards Earth Syst. Sci., 11, 3181-3195.
58. WÜNSCH, A., HERRMANN, U., KREIBICH, H. & THIEKEN, A. 2009. The Role of Disaggregation of Asset Values in Flood Loss Estimation: A Comparison of Different Modeling Approaches at the Mulde River, Germany. Environmental Management, 44, 524-541.
59. XIA, J., FALCONER, R. A., LIN, B. & TAN, G. 2011. Numerical assessment of flood hazard risk to people and vehicles in flash floods. Environmental Modelling & Software, 26, 987-998.